Preprint LNS-99-288, NSF-PT-99-1, UR-1569

Neutrino Mass and Oscillation

Peter Fisher
Massachusetts Institute of Technology, Department of Physics, Cambridge, MA 02192

Boris Kayser
National Science Foundation, Division of Physics, Arlington, VA 22230

Kevin S. McFarland
University of Rochester, Department of Physics and Astronomy, Rochester, NY 14627

arXiv:hep-ph/9906244v1 4 Jun 1999

KEYWORDS: neutrino, neutrino mass, neutrino oscillations

ABSTRACT: The question of neutrino mass is one of the major riddles in particle physics. Recently, strong evidence that neutrinos have nonzero masses has been found. While tiny, these masses could be large enough to contribute significantly to the mass density of the universe. The evidence for nonvanishing neutrino masses is based on the apparent observation of neutrino oscillation—the transformation of a neutrino of one type or "flavor" into one of another. We explain the physics of neutrino oscillation, and review and weigh the evidence that it actually occurs in nature. We also discuss the constraints on neutrino mass from cosmology and from experiments with negative results. After presenting illustrative neutrino mass spectra suggested by the present data, we consider how near- and far-future experiments can further illuminate the nature of neutrinos and their masses.

CONTENTS

INTRODUCTION 2

THE EXPECTATION THAT NEUTRINOS HAVE MASS 3

NEUTRINO OSCILLATION 3
Oscillation in Vacuum 4
Flavor Transitions in Matter 7
Types of Neutrino Oscillation Experiments 8

THE OBSERVED EVIDENCE AND HINTS OF NEUTRINO OSCILLATION . . 9
Atmospheric Neutrinos 9
Solar Neutrinos 17
The LSND Experiment 21

A COSMOLOGICAL CONSTRAINT ON NEUTRINO MASS 24

NEGATIVE SEARCHES FOR NEUTRINO MASS 24
Reactor Oscillation Searches 25
Accelerator Oscillation Searches 27
Kinematic Searches for Mass 29
Double Beta Decay 31

NEUTRINO MASS SCENARIOS 33

CONCLUSIONS 36

1 INTRODUCTION

Neutrinos are among the most abundant particles in the universe. Indeed, even within a single human being, there are more than 10^7 neutrinos left over from the Big Bang. In addition, passing through each person on earth every second are some 10^{14} neutrinos from the sun, another 10^3 neutrinos made in the earth's atmosphere by cosmic rays, and additional neutrinos from other natural and man-made sources. Evidently, neutrinos are very common in the universe, and very commonly encountered by people. Thus, it would be very nice to know something about them.

It has long been known that neutrinos are very light. However, it has not been known whether they are completely massless, or have small but nonzero masses. The answer to this question has major consequences, both for physics and for astrophysics. If the neutrino masses are very small but nonvanishing, then they are probably caused by new physics beyond the realm of the highly successful Standard Model of the weak and electromagnetic interactions. Measured values of the masses would be a clue to the nature of the new physics. In addition, because neutrinos are so abundant in the universe, even tiny nonzero neutrino masses can result in an important neutrino contribution to the mass density of the universe.

Recently, strong evidence that neutrinos do have nonzero masses has at long last been found. This evidence stems from the apparent observation that a neutrino of one type or "flavor", such as a muon neutrino, can metamorphose into a neutrino of another flavor, such as a tau neutrino. This metamorphosis, known as neutrino oscillation, implies neutrino mass, as we shall discuss.

Three hints that neutrinos oscillate have been observed. The first—the behavior of neutrinos produced in the earth's atmosphere by cosmic rays—provides rather convincing evidence of oscillation. The second—the observed fluxes of neutrinos from the sun—provides a strong further hint of it. The third—the behavior of neutrinos in a beam at Los Alamos—provides an additional but unconfirmed hint.

In this article, we will briefly review the physics of neutrino mass and oscillation, and then discuss and critique the three hints that neutrinos actually oscillate. Next, we will indicate the bounds placed on neutrino mass by astrophysics and by various laboratory experiments with negative results. Then, we will describe several illustrative neutrino mass scenarios suggested by the observed oscillation hints and consistent with the existing bounds. Finally, we will conclude by discussing the future steps which need to be taken to test the three existing hints of oscillation, and to learn more about the nature of neutrinos and their masses.

2 THE EXPECTATION THAT NEUTRINOS HAVE MASS

Over the years, numerous experiments have sought evidence of neutrino mass. This extensive search has been driven, in part, by the fact that from a theoretical perspective, it is natural to expect that neutrinos do have nonvanishing masses. Unlike photons, neutrinos are not required to be massless by gauge invariance or any other symmetry principle. Moreover, neutrinos appear to be closely related to the charged leptons and the quarks, all of which certainly have nonvanishing masses. In the Grand Unified Theories, which unify the weak, electromagnetic, and strong interactions, this relation takes the form of the placement of each neutrino in a multiplet together with at least one charged lepton, one positively-charged quark, and one negatively-charged quark. Apart from the neutrino, every member of this multiplet is known to be massive. Thus the neutrino would have to be an exceptional member of the multiplet to be massless.

Assuming that neutrinos do have mass, we have to understand why they are nevertheless so much lighter than the charged leptons and quarks. The most popular explanation of this fact is the "see-saw mechanism" [1]. To understand how this mechanism works, let us recall that, unlike charged particles, neutrinos may be their own antiparticles. A neutrino which is its own antiparticle consists of just two states with a common mass: one with spin up and one with spin down. Such a neutrino is called a Majorana neutrino. By contrast, a neutrino which is distinct from its antiparticle consists of four states with a common mass: the spin-up and spin-down neutrino, plus the spin-up and spin-down antineutrino. This collection of four states is called a Dirac neutrino. In the see-saw mechanism, a four-state Dirac neutrino $\mathcal{N}^D$ of mass M^D gets split by "Majorana mass terms" into a pair of two-state Majorana neutrinos. One of the latter neutrinos, ν^M, has a small mass M_ν and is identified as one of the observed light neutrinos. The other, N^M, has a large mass M_N reflecting the high mass scale of some new physics beyond the Standard Model, and has not been observed. The character of the breakup of $\mathcal{N}^D$ into ν^M and N^M is such that $M_\nu M_N \cong M_D^2$. Now, it is reasonable to expect that the mass M_D of the Dirac particle $\mathcal{N}^D$ is of the same order as the typical mass, $M_{\ell \text{ or } q}$, of the charged leptons ℓ and quarks q, since the latter are Dirac particles as well. Then, $M_\nu M_N \sim M_{\ell \text{ or } q}^2$. With $M_{\ell \text{ or } q}$ a typical charged lepton or quark mass and M_N very large, this "see-saw relation" explains why M_ν is very small. Very importantly, the see-saw mechanism predicts that neutrinos are Majorana particles.

In a typical model, the heavy Majorana neutral lepton N^M participates in some hypothetical feeble interaction beyond the familiar weak interaction. However, it does not participate in the weak interaction itself. For this reason, it (and any other neutrino which is free of normal weak interactions) is sometimes referred to as a "sterile neutrino".

3 NEUTRINO OSCILLATION

In the quest for evidence of neutrino mass, the experiments which currently can reveal the smallest neutrino masses are those which search for neutrino oscillation. Let us briefly recall the physics of this process, starting with oscillation in empty space.

3.1 Oscillation in Vacuum

We shall denote by "ℓ" the charged lepton of flavor $\ell = e$, μ, or τ. Associated with a charged lepton ℓ of a given flavor is a neutrino, ν_ℓ, of the same flavor. The meaning of this association is that when a neutrino of a given flavor interacts with matter and produces a charged lepton, this charged lepton always has the same flavor as the neutrino: ν_e produces an e, ν_μ a μ, and ν_τ a τ. Similarly, when a reaction creates a charged lepton and an accompanying neutrino, the latter two particles are of the same flavor.

If neutrinos have masses, then a neutrino of definite flavor, ν_ℓ, need not be a mass eigenstate. Indeed, if leptons behave as quarks do, then ν_ℓ is a coherent superposition of mass eigenstates, given by

$$|\,\nu_\ell\rangle = \sum_m U_{\ell m}\,|\,\nu_m\rangle. \tag{1}$$

Here, the ν_m are the mass eigenstates. There are at least three of them, and perhaps more. The coefficients $U_{\ell m}$ form a matrix U known as the leptonic mixing matrix. According to the Standard Model (SM), extended to include neutrino masses, U is unitary.

The fact that a neutrino of definite flavor is a superposition of several mass eigenstates, whose differing masses cause them to propagate differently, leads to *neutrino oscillation in vacuum*—the transformation of a neutrino of one flavor into one of a different flavor as the neutrino moves through empty space. The amplitude for the transformation $\nu_\ell \to \nu_{\ell'}$ is given by

$$A(\nu_\ell \to \nu_{\ell'}) = \sum_m A(\nu_\ell \text{ is } \nu_m)\, A(\nu_m \text{ propagates})\, A(\nu_m \text{ is } \nu_{\ell'})\ . \tag{2}$$

Here, A denotes an amplitude. From Eq. (1), $A(\nu_\ell \text{ is } \nu_m) = U_{\ell m}$, and from its inverse, $A(\nu_m \text{ is } \nu_{\ell'}) = U^*_{\ell' m}$. It is not difficult to show that if the neutrino has energy E, if it propagates for a distance L between its production and detection, and if ν_m has mass M_m, then $A(\nu_m \text{ propagates}) = exp(-i\frac{M_m^2}{2}\frac{L}{E})$ [2, 3, 4]. Inserting these amplitudes into Eq. (2), we have

$$A(\nu_\ell \to \nu_{\ell'}) = \sum_m U_{\ell m} e^{-i\frac{M_m^2}{2}\frac{L}{E}} U^*_{\ell' m}. \tag{3}$$

The probability $P(\nu_\ell \to \nu_{\ell'})$ for a neutrino of flavor ℓ to oscillate in vacuum into one of flavor ℓ' is then just the square of this amplitude.

Note from Eq. (3) that oscillation from one flavor to another does require neutrino mass. If all the masses M_m vanish, then, since U is unitary, Eq. (3) implies that $A(\nu_\ell \to \nu_{\ell'}) = \sum_m U_{\ell m} U^*_{\ell' m} = \delta_{\ell\ell\prime}$.

The quantum mechanics of neutrino oscillation is both fascinating and subtle [5]. It continues to be explored [6].

If only two flavors, ℓ and $\ell' \neq \ell$, mix appreciably, U takes the form

$$U = \begin{pmatrix} \cos\theta & e^{i\delta}\sin\theta \\ -e^{-i\delta}\sin\theta & \cos\theta \end{pmatrix}\ . \tag{4}$$

Here, θ is a mixing angle, and δ is a phase. Inserting Eq. (4) into Eq. (3), and supplying the factors of $\hbar$ and c which we have been omitting, we find that

$$P(\nu_\ell \to \nu_{\ell' \neq \ell}) = \sin^2 2\theta\, \sin^2\left[1.27\,\delta M^2(\mathrm{eV}^2)\frac{L(\mathrm{km})}{E(\mathrm{GeV})}\right]. \tag{5}$$

Here, $\delta M^2 \equiv M_2^2 - M_1^2$ is the splitting between the squared masses of ν_1 and ν_2, the two neutrino mass eigenstates which make up ν_ℓ and $\nu_{\ell'}$.

As we see from Eq. (5), the oscillation probability $P(\nu_\ell \to \nu_{\ell \neq \ell'})$ is not appreciable unless $\delta M^2(\mathrm{eV}^2)\, L(\mathrm{km})/E(\mathrm{GeV})$ is of order unity or larger. Thus, an experiment characterized by a given $L(\mathrm{km})/E(\mathrm{GeV})$ will be able to probe neutrino mass splittings $\delta M^2(\mathrm{eV}^2) \gtrsim [L(\mathrm{km})/E(\mathrm{GeV})]^{-1}$. By making L/E large enough, one can probe very tiny values of δM^2. Herein lies the power of neutrino oscillation searches.

Neutrino oscillation experiments are very commonly analyzed assuming that the oscillation probability is correctly described by Eq. (5). However, this equation was derived assuming that only two neutrinos mix appreciably. If three or more mix, Eq. (5) may not hold. Nevertheless, there are interesting situations in which, even though more than two neutrinos are mixing, Eq. (5), with the meaning of "$\sin^2 2\theta$" and "δM^2" slightly modified, does hold. A second point concerns the possibility of CP violation. Assuming that the observed CP-violating effects in K meson decays are due to Standard Model physics, there must be CP-violating phase factors in the quark analogue of the leptonic mixing matrix U. Thus, it is natural to expect that there are CP-violating phases in U as well. These phases could lead to CP-violating effects such as $P(\bar{\nu}_\mu \to \bar{\nu}_e) \neq P(\nu_\mu \to \nu_e)$ [7]. However, some neutrino oscillation measurements are completely insensitive to any CP-violating phases in U.

An example which nicely illustrates both of these points is the scenario in which there are three neutrino mass eigenstates, with two of them much lighter than the third. That is, $M_{1,2} \ll M_3$. Imagine, now, that one searches for ${}^{(-)}\nu_\ell \to {}^{(-)}\nu_{\ell' \neq \ell}$ in an experiment with L/E such that $M_3^2(L/E) \sim 1$, so that $M_{1,2}^2(L/E) \ll 1$. Then, in Eq. (3) for $A(\nu_\ell \to \nu_{\ell'})$, we have $\exp(-iM_{1,2}^2 L/2E) \cong 1$. Thus, since the unitarity of U requires that $U_{\ell 1} U_{\ell' 1}^* + U_{\ell 2} U_{\ell' 2}^* = -U_{\ell 3} U_{\ell' 3}^*$, Eq. (3) yields $A(\nu_\ell \to \nu_{\ell'}) = U_{\ell 3} U_{\ell' 3}^* [-1 + \exp(-iM_3^2 L/2E)]$. Squaring, and including the factors of $\hbar$ and c, we have

$$P(\nu_\ell \to \nu_{\ell' \neq \ell}) = |2\, U_{\ell 3} U_{\ell' 3}|^2 \sin^2 \left[1.27\, M_3^2(\mathrm{eV}^2) \frac{L(\mathrm{km})}{E(\mathrm{GeV})} \right]. \qquad (6)$$

This oscillation probability has exactly the same mathematical form as the two-neutrino formula, Eq. (5), but with the role of "$\sin^2 2\theta$" played by $|2U_{\ell 3} U_{\ell' 3}|^2$, and that of "$\delta M^2$" played by M_3^2. Thus, even when more than two neutrinos participate in the mixing, describing the data of an oscillation experiment using the two-neutrino formula of Eq. (5) may still be a valid procedure. Turning to the question of whether the experiment under discussion can see CP violation, we recall that CPT invariance implies that one can obtain $P(\bar{\nu}_\ell \to \bar{\nu}_{\ell'})$ from $P(\nu_\ell \to \nu_{\ell'})$ by simply replacing U by U^* [7]. Since this replacement does not affect Eq. (6) at all, we see that in our experiment, $P(\bar{\nu}_\ell \to \bar{\nu}_{\ell' \neq \ell})$ is forced to be the same as $P(\nu_\ell \to \nu_{\ell' \neq \ell})$, even if CP-violating phases are present in U. Our experiment cannot uncover these phases [8].

The presence of CP-violating phases could, however, be revealed by an experiment with L/E big enough so that even $M_{1,2}^2(L/E) \gtrsim 1$. To see this, we note that when there are three flavors and three neutrino mass eigenstates, Eq. (3) and the rule that $P(\bar{\nu}_\ell \to \bar{\nu}_{\ell'})$ is the same as $P(\nu_\ell \to \nu_{\ell'})$ except that U is replaced by U^* imply that

$$P(\nu_\ell \to \nu_{\ell' \neq \ell}) - P(\bar{\nu}_\ell \to \bar{\nu}_{\ell' \neq \ell}) = 4\, \Im\mathrm{m}(U_{\ell 1} U_{\ell' 1}^* U_{\ell 2}^* U_{\ell' 2})(s_{12} + s_{23} + s_{31})\,. \qquad (7)$$

Here, $s_{ij} \equiv \sin(\delta M^2_{ij} L/2E)$, where $\delta M^2_{ij} \equiv M^2_i - M^2_j$. If U contains CP-violating phase factors, the quantity $\Im\mathrm{m}(U_{\ell 1} U^*_{\ell' 1} U^*_{\ell 2} U_{\ell' 2})$ will be nonvanishing [9]. Thus, from Eq. (7) we see that, in an experiment in which $\delta M^2_{ij} L/2E$ is not tiny compared to unity for any $i \neq j$, the CP-violating asymmetry $P(\nu_\ell \to \nu_{\ell' \neq \ell}) - P(\bar{\nu}_\ell \to \bar{\nu}_{\ell' \neq \ell}) \equiv A_{\rm CP}(\ell\ell')$ will be nonvanishing as well. Interestingly, the unitarity of U is readily shown to imply that $A_{\rm CP}(\ell\ell')$, as given by Eq. (7), has the same value for $\ell\ell' = e\mu,\ \mu\tau$, or τe. Furthermore, Eq. (7) obviously implies that $A_{\rm CP}(\ell'\ell) = -A_{\rm CP}(\ell\ell')$. Thus, when there are only three neutrinos, all the CP asymmetries $A_{\rm CP}(\ell\ell')$ are equal to within a sign. However, if, say, $\delta M^2_{12} L/2E \ll 1$, then $s_{12} + s_{23} + s_{31} \cong 0$, and all the asymmetries $A_{\rm CP}(\ell\ell')$ disappear. This is the situation we encountered in the example we just discussed. Obviously, the CP asymmetries also disappear if $\delta M^2_{23} L/2E$ or $\delta M^2_{31} L/2E$ is much smaller than unity.

In Section 2, we saw that the see-saw mechanism predicts the existence of *very heavy* neutral leptons in addition to the observed three light neutrinos. It may be that there are also *light* neutrinos in addition to the observed ν_e, ν_μ, and ν_τ. It is known that, should there be any such additional light neutrinos, the weak boson Z does not couple to them [10]. This means that these additional neutrinos do not participate in the normal weak interactions of the SM. That is, they are what are called "sterile" neutrinos.

If there do exist light sterile neutrinos, then any of the weak-interaction "active" neutrinos, ν_e, ν_μ, or ν_τ, can oscillate, not only into another active neutrino, but into a sterile neutrino as well. The mathematics of neutrino oscillation when sterile neutrinos are involved is the same as when they are not. One simply increases the number of neutrino flavors, the number of neutrino mass eigenstates, and the consequent size of the mixing matrix U, to accommodate the new neutrinos of sterile flavor.

Owing to the special nature of the SM weak currents which produce and absorb neutrinos, many neutrino processes are insensitive to whether the neutrinos are Dirac or Majorana particles [11]. By and large, neutrino oscillation is insensitive as well. However, if the neutrino mass eigenstates are Majorana particles, then in addition to the oscillation of one neutrino flavor into another, which we have been discussing, we can also have the oscillation of a neutrino into an antineutrino. That is, a neutrino which in interaction with matter produces a negatively-charged lepton ℓ^- (conventionally called a "lepton") can become one which produces a positively-charged lepton ℓ^+ (conventionally called an "antilepton"). There are several different varieties of this $\nu \to \bar{\nu}$ oscillation. To understand these varieties, let us recall that, irrespective of whether neutrinos are of Majorana or Dirac character, neutrino interactions obey certain helicity rules [11]. When the SM weak interactions produce an $\ell^+(\ell^-)$, the accompanying neutrino or antineutrino almost (but not quite) certainly has negative (positive) helicity. The amplitude for it to have positive (negative) helicity is suppressed, and is only of order M/E, where M and E are, respectively, the mass and energy of the neutrino. Correspondingly, when the SM weak interactions absorb a neutrino or antineutrino to produce an $\ell^-(\ell^+)$, the absorbed particle must have negative (positive) helicity. The amplitude for it to be absorbed and produce a lepton of the desired charge if it has the wrong helicity is, again, only of order M/E. However, these suppressed amplitudes are not zero.

When neutrinos are Dirac particles, there is a conserved lepton number L, with $L(\ell^-) = L(\nu) = -L(\ell^+) = -L(\bar{\nu}) = +1$. Conservation of L prevents a

neutrino from being born in association with an ℓ^+ and then interacting to make a second ℓ^+ instead of an ℓ^-. But when neutrinos are Majorana particles, no such conservation law stands in the way. The neutrino need only have the proper helicity. Now, as has been stated, when a "neutrino" is born in association with an ℓ^+, this neutrino, while dominantly of negative helicity, has a small component, of order M/E, with positive helicity. This small component has the right helicity to make an ℓ^+ when interacting with matter. Since a particle whose interaction with matter yields an ℓ^+ is customarily called an "antineutrino", we would say that the particle born as a ν became a $\bar{\nu}$. However, it is probably not too accurate to say the ν "oscillated" into a $\bar{\nu}$, since a small piece of it had the correct helicity to act as a $\bar{\nu}$ right from the moment of birth, without having to travel any distance at all. This is the first variety of $\nu \to \bar{\nu}$ "oscillation".

A quite different kind of $\nu \leftrightarrow \bar{\nu}$ oscillation is the neutrino analogue of $B^o \leftrightarrow \bar{B}^o$ meson oscillation. Like the latter, which has been observed [12], this would be a genuine oscillation with distance. It is sometimes referred to as 2nd class oscillation [13]. To illustrate how this type of oscillation works, let us neglect intergenerational mixing, and imagine that the electron neutrino with negative helicity, $\nu_e^\downarrow$, and its charge conjugate, the electron antineutrino with negative helicity $\bar{\nu}_e^\downarrow$, are orthogonal linear combinations of two underlying Majorana mass eigenstates. Here the arrows indicate the helicity. This situation is analogous to the one in the $B^o - \bar{B}^o$ system, where B^o and $\bar{B}^o$ are orthogonal linear combinations of two mass eigenstates. Just as a B meson born as a B^o then oscillates between B^o and $\bar{B}^o$ states, so a neutrino born as a $\nu_e^\downarrow$ would oscillate between $\nu_e^\downarrow$ and $\bar{\nu}_e^\downarrow$. Note that the latter oscillation necessarily connects two states of the same helicity, since the angular momentum of a neutrino in vacuum is conserved. Now, a $\bar{B}^o$ participates in SM interactions, but a $\bar{\nu}_e^\downarrow$ does not, being of the wrong helicity to do so. That is, this brand of "$\nu \leftrightarrow \bar{\nu}$ oscillation" turns an active neutrino, $\nu_e^\downarrow$, into a sterile one, $\bar{\nu}_e^\downarrow$. In particular, this sterile neutrino does not interact to produce a positron, as a $\bar{\nu}_e^\uparrow$ would. In an experiment starting with a ν_e beam, $\nu_e^\downarrow \to \bar{\nu}_e^\downarrow$ would be marked by a disappearance of some (possibly large) fraction of the original ν_e flux, but without the appearance of a corresponding flux of new particles capable of interacting to produce a charged lepton of any charge or flavor. Of course, with probability $\sim (M/E)^2$, a $\bar{\nu}_e^\downarrow$ can indeed produce an e^+, but this is a very small effect. Neutrino-antineutrino oscillation is a potentially very interesting effect, but estimates of its experimental visibility are discouraging [14].

3.2 Flavor Transitions in Matter

When a neutrino propagates through matter, rather than through a vacuum, its ability to change its flavor can be greatly enhanced by its interaction with the surrounding medium. This phenomenon, known as the Mikheyev-Smirnov-Wolfenstein (MSW) effect [15], results from weak forward coherent scattering from electrons, and may play a very important role in the behavior of the solar neutrinos (see Section 4.2). A solar neutrino is created as a ν_e in the core of the sun by nuclear processes. The solar neutrino detectors presently operating on earth can detect a ν_e, but are completely, or at least largely, insensitive to neutrinos of other flavors. However, as the solar neutrino born as a ν_e journeys outward from the solar core through solar material, the MSW effect can potentially convert it into a neutrino ν_x of muon, tau, or even sterile flavor. It would

then be undetectable in the present detectors. Thus, the solar neutrino flux observed by these detectors would be less than that predicted when one does not take this MSW flavor conversion into account.

Like neutrino oscillation in vacuum, MSW flavor conversion requires neutrino mass. Without going through the physics of the MSW effect in detail, let us recall enough of it to see how much mass it requires.

The MSW effect converts a ν_e into a ν_x ($= \nu_\mu, \nu_\tau$, or $\nu_{\rm sterile}$) as a result of a crossing, somewhere in the sun, of the ν_e and ν_x energy levels. Neglecting neutrino mixing, the total energy of a ν_e of mass M_{ν_e} and momentum p in the sun is $\sqrt{p^2 + M_{\nu_e}^2} + \sqrt{2} G_F N_e$. Here, G_F is the Fermi coupling constant, and N_e is the electron density at the location of the neutrino. The term $\sqrt{p^2 + M_{\nu_e}^2}$ is the energy the ν_e would have in empty space, and the term $\sqrt{2} G_F N_e$ is an interaction energy arising from the W-boson exchange interaction between the ν_e and solar electrons. We have neglected a small Z-boson exchange interaction. Now, a ν_x ($= \nu_\mu, \nu_\tau$, or $\nu_{\rm sterile}$) does not have a W-boson exchange interaction with electrons. Thus, neglecting the small Z-boson exchange interaction once again, the total energy of a ν_x of mass M_{ν_x} and the same momentum p as before is simply $\sqrt{p^2 + M_{\nu_x}^2}$. The condition that the ν_e and ν_x energy levels cross is then

$$\sqrt{p^2 + M_{\nu_x}^2} \cong \sqrt{p^2 + M_{\nu_e}^2} + \sqrt{2} G_F N_e \; . \tag{8}$$

Taking for N_e a characteristic solar electron density, $\sim 10^{26}$/cc, and for p a characteristic solar neutrino momentum, ~ 1 MeV, we find that if this level-crossing condition is to be satisfied, we must have

$$M_{\nu_x}^2 - M_{\nu_e}^2 \equiv \delta M_{\nu_x \nu_e}^2 \sim 10^{-5} {\rm eV}^2 \; . \tag{9}$$

This is the amount of mass (splitting) required by the MSW effect. Note, in particular, that the MSW effect does require nonzero neutrino mass. [1]

3.3 Types of Neutrino Oscillation Experiments

Neutrino flavor oscillation experiments fall crudely into two categories: disappearance experiments, and appearance experiments. If an experimenter creates a beam of neutrinos of lepton flavor ℓ, then in a disappearance experiment, he or she will search for the absence of some of the ν_ℓ flux known to be present in the initial beam. In an appearance experiment, he or she will seek the appearance of neutrinos $\nu_{\ell' \neq \ell}$. The appearance of a lepton flavor not present in the original beam is often a more convincing signal of oscillation than is the disappearance of some fraction of a neutrino beam whose total flux may be uncertain. However, it may be that in some cases neutrino oscillations convert active neutrinos into sterile ones. To discover this, an experimenter would have to demonstrate both the disappearance of the original active flavor and the non-appearance of any new active flavor in its stead.

Experiments seeking neutrino flavor oscillations typically use charged-current neutrino interactions ($\nu_\ell + A \to \ell + B$) to tag the flavor of the observed neutrinos.

[1] Of course, if there should exist flavor-changing neutrino interactions such as ν_e + nucleon $\to \nu_\mu$ + nucleon, then a neutrino could change flavor in matter even in the absence of neutrino mass. However, we assume that, as in the SM, there are no neutrino-flavor-changing interactions. Then flavor conversion requires neutrino mass.

Experiments with low neutrino energy, which are desirable to increase L/E for the purposes of probing low δM^2, are often unable to use this technique because of the lack of energy necessary to produce the massive charged lepton. Observations of neutral-current neutrino interactions ($\nu_\ell + A \rightarrow \nu_\ell + B$) are important probes of the sterile neutrino hypothesis, since neutral-current interactions would be absent for sterile neutrinos but present for active neutrinos even when the related charged-current interactions are suppressed by the charged lepton mass.

A particular case of interest occurs when backgrounds and intensities are low, such as in many "long-baseline" (large L) experiments. Appearance experiments have sensitivities which scale with $N \times P$, where N is the number of neutrinos expected in the detector and P is the probability of flavor oscillation. However, disappearance experiments have sensitivities which scale as $P\sqrt{N/(1-P)}$, and are therefore often less powerful at low mixing angle in the case of transition from $\nu_{\rm active} \rightarrow \nu'_{\rm active}$.

Interestingly, CP violation in neutrino oscillation could never be seen in a disappearance experiment. Such an experiment simply measures the probability $P(\nu_\ell \rightarrow \nu_\ell)$ that a neutrino retains its original flavor. Violation of CP would be signalled by $P(\bar{\nu}_\ell \rightarrow \bar{\nu}_\ell) \neq P(\nu_\ell \rightarrow \nu_\ell)$. However, one can show that CPT invariance demands that $P(\bar{\nu}_\ell \rightarrow \overline{\nu}_\ell) = P(\nu_\ell \rightarrow \nu_\ell)$.

In order to establish oscillation as the correct explanation of an observed phenomenon, it is desirable to observe the characteristic variation in neutrino beam composition with L/E. This may appear as a spectral distortion of a wideband source of neutrinos or as a change in observed appearance rates as L/E varies in a narrowband source.

4 THE OBSERVED EVIDENCE AND HINTS OF NEUTRINO OSCILLATION

4.1 Atmospheric Neutrinos

Atmospheric neutrinos are produced by interactions of cosmic ray protons with air nuclei in the earth's atmosphere via the reaction chain

$$p + N \rightarrow \pi^\pm + X \tag{10}$$

$$\pi^\pm \rightarrow \mu^\pm + \nu_\mu(\overline{\nu}_\mu) \tag{11}$$

$$\mu^\pm \rightarrow e^\pm + \nu_e(\overline{\nu}_e) + \overline{\nu}_\mu(\nu_\mu). \tag{12}$$

From simple counting the flavor ratio resulting from this chain is

$$R_{\mu/e} = \frac{N(\nu_\mu + \overline{\nu}_\mu)}{N(\nu_e + \overline{\nu}_e)} \sim 2. \tag{13}$$

A more sophisticated calculation changes this ratio somewhat, but calculations from different groups[16] are consistent at the 5% level. The absolute fluxes are believed to be known at the 20% level. This makes neutrinos produced in the atmosphere a potentially good place to look for oscillation effects: the ratio between species is reasonably well known even though the absolute fluxes are not.

Generally, an oscillation effect would show up as a variation of the above ratio from the calculated value of approximately 2. Detailed calculations of flavor ratios are used to account for detector effects, such as energy thresholds and acceptances which vary from experiment to experiment and deviations from $R_{\mu/e} = 2$ at

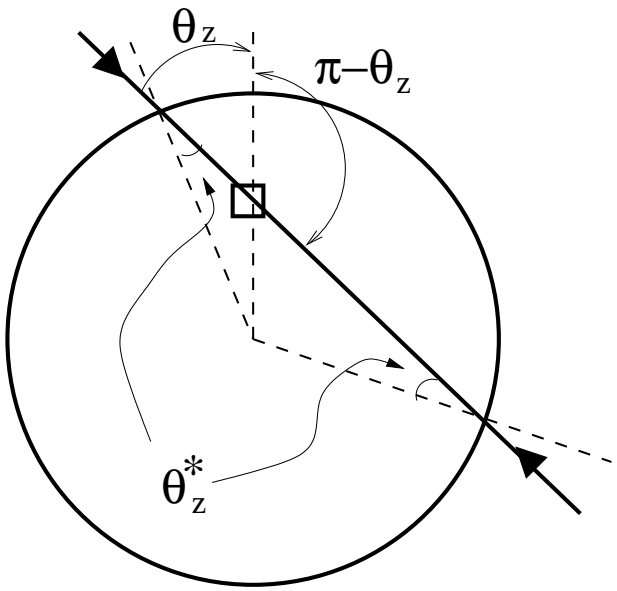

Figure 1: Atmospheric neutrinos incident on an underground detector from zenith angles θ_Z and $\pi - \theta_Z$. The large circle is the earth, and the black square the detector. The various dashed lines intersect at the center of the earth. The neutrinos travel as shown by the arrows along the solid line from their points of origin just above the earth's surface to the detector.

higher neutrino energies. Conventionally, experimenters report the ratio between the measured value of the quotient in Eq. (13), and its predicted value based on a Monte Carlo simulation:

$$R_{\rm Data/MC} = \frac{\left[N(\nu_\mu + \overline{\nu}_\mu)/N(\nu_e + \overline{\nu}_e)\right]_{\rm Data}}{\left[N(\nu_\mu + \overline{\nu}_\mu)/N(\nu_e + \overline{\nu}_e)\right]_{\rm MC}} \ . \tag{14}$$

This "ratio of ratios" should be unity if there are no neutrino oscillations and if detector effects and backgrounds are correctly modeled. If ν_μ flavor oscillations occur, $R_{\mu/e}$ would be less than two and $R_{\rm Data/MC}$ would be less than one.

The zenith angle distribution of neutrino events of a given flavor provides a second, more sensitive, method of detecting oscillations which is less dependent on theoretical input. Neutrinos produced in the atmosphere just above the detector will have a shorter flight path (20 km) than neutrinos produced on the opposite side of the earth, which travel up to 13,000 km before detection. Thus, the oscillation baseline varies with the zenith angle θ_Z. In the absence of oscillations, the zenith angle distribution will be up-down symmetric to a good approximation, and any deviation from this symmetry will indicate a change in the neutrino flux during passage through the earth. As this point may not be immediately clear, we give the argument in detail below.

Suppose that neutrinos do not oscillate. More generally, suppose that the number of neutrinos of a given flavor does not change for any reason as the neutrinos travel from their points of birth to the detector. Then, at neutrino energies above a few GeV, where geomagnetic effects can be neglected, the detected flux of neutrinos of a given flavor coming from zenith angle θ_Z must be equal to that coming from angle $\pi - \theta_Z$. To see why, consider Figure 1.

Measurements have found that above a few GeV the cosmic ray flux which

produces the atmospheric neutrinos is isotropic [17]. Thus, neutrinos are being created in equal numbers per unit area and time everywhere around the earth in Figure 1. In addition, the angular distribution of the produced neutrinos, relative to the local downward-pointing vertical, is the same around the world. We shall call this angular distribution $D(\theta_Z^*)$, where θ_Z^* is the angle between the momentum of the neutrino and the downward vertical. Consider, now, the downward flux of neutrinos incident on the detector from a small solid angle $\Delta\Omega$ at zenith angle θ_Z. Let us compare this to the corresponding upward flux from the same size solid angle at $\pi - \theta_Z$. Note from Figure 1 that the angle θ_Z^* between the momentum the neutrinos must have to reach the detector and the downward vertical at the neutrino production point is the same for the neutrinos coming from $\pi - \theta_Z$ as for those coming from θ_Z. Thus, $D(\theta_Z^*)$ has the same value for both. For a $\Delta\Omega$ of given size, the surface area of the region of atmosphere that contributes neutrinos is proportional to ℓ^2, where ℓ is the distance from the detector to the contributing region. This effect would appear to favor the upward-going neutrinos from the distant source at $\pi - \theta_Z$ over the downward-going ones from the nearby source at θ_Z. However, for the neutrinos coming from a tiny area da of fixed size within the source region, the solid angle subtended by the detector falls off as $1/\ell^2$. Thus, when one integrates over the contributing source region, the factors of ℓ^2 cancel out, and neither the upward- nor downward-going neutrinos are favored. Finally, since the source region of atmosphere is not perpendicular to the line connecting it to the detector, for given $\Delta\Omega$ the size of this region is enhanced by a factor of $\sec\theta_Z^*$. However, since θ_Z^* is the same for the neutrinos from θ_Z and from $\pi - \theta_Z$, this factor, like all the others, does not favor either of these neutrinos.

The conclusion is that, per unit solid angle, the fluxes of neutrinos of a given flavor incident on the detector from directions θ_Z and $\pi - \theta_Z$ must be equal. If they are not, then the number of neutrinos of this flavor must change as the neutrinos journey from their points of origin to the detector. Most likely, the change is due to vacuum neutrino oscillation, although one must be careful to consider other possibilities, such as the decay of neutrinos of one flavor into those of another[18].

4.1.1 Experimental Results

The first generation detectors which studied atmospheric neutrinos, NUSEX[19], Soudan[20], IMB[21], Frejus[22] and Kamiokande[23], were originally designed to search for proton decay. All are deep underground to reduce backgrounds from cosmic rays, all are very massive in order to be sensitive to proton lifetimes of order 10^{32} yr and designed in order to minimize backgrounds from radioactive substances. These characteristics make them ideal for the detection of both solar and atmospheric neutrinos: the neutrino flux from cosmic ray interactions in the atmosphere is expected to be $\sim 10^9$ m^{-2}-sr^{-1}-(100 MeV)$^{-1}$-yr^{-1}, at 1 GeV, so there are ~ 50 reactions per kiloton of target mass per year.

For the second generation of detectors, Soudan II[20], Kamiokande III[24] and IMB-3[21], the key improvement was lowering of the energy threshold of the detector trigger. Generally, this required the use of lower background materials and noise reduction in the detector systems as well as the ability to handle higher data rates. SuperKamiokande[25] represents the third generation of proton decay experiments with neutrino detection placed on an equal footing with proton decay. SuperKamiokande's larger fiducial volume not only means a higher counting rate

from neutrino interactions, but the ability to fully contain a larger fraction of the final state products from the neutrino interactions.

The large underground detectors are of two types: water Čerenkov (IMB-3, Kamiokande and SuperKamiokande), which use water as the target and measure the Čerenkov light cone to determine a particle's velocity and direction, and tracking detectors (Soudan, Frejus, NUSEX and MACRO), which use dense material as a target and sampling detectors to identify the final state lepton.

The most sensitive result comes from SuperKamiokande, the latest of the water Čerenkov detectors, and we describe it in some detail. A particle moving through a medium of index of refraction n with a velocity greater than c/n will radiate photons into a forward cone of opening angle $\cos\theta_c = 1/n\beta$. For ultra-relativistic particles in water, the Čerenkov angle is $\theta_c = 41.7^\circ$, and a charged particle moving through water will generate around nine photo-electrons per MeV of deposited energy. The arrival time of the photons at the photon detectors allows the reconstruction of the Čerenkov cone and hence the velocity and direction of the charged particle. The 200 ps timing resolution of the photon detectors gives a vertex resolution of 30 cm. The total path length gives the total energy with a resolution of $2.5\%/\sqrt{E(\mathrm{GeV})} \pm 0.5\%$ for electrons and 3% for muons.

Two key ingredients make measurements of atmospheric neutrinos possible in water Čerenkov detectors. First, even at a depth of 1000 meters (equivalent to 3000 meters of water), the cosmic muon flux is $10^8\mu$/year in SuperKamiokande compared to the observed change in the flux (see below), which is around 150 events for a year of running. Requiring tracks to originate at least 2 m from the surface of the detector reduces the accidental flux by a factor of 10^9 for the fiducial mass of 22 kilotons of this detector [28]. Second, the very large number of Čerenkov photons allows discrimination between electrons and muons based on the larger multiple scattering of the electrons owing to their low mass[26]. The higher multiple scattering of electrons leads to a fuzzier Čerenkov ring image; measuring the sharpness of this image allows discrimination between electrons and muons with less than 1% confusion.

Fully contained events are classified according to their visible energy ("sub-GeV" for $E_{\mathrm{vis}} < 1.33$GeV, "multi-GeV" for $E_{\mathrm{vis}} > 1.33$ GeV) and the number of reconstructed Čerenkov rings ("single-ring" for one reconstructed ring, "multi-ring" for two or more). Single ring events are further classified based on whether the ring originates from an electron ("e-like") or a muon ("μ-like"). Identification of the final state lepton is not possible for multi-ring events. Events in which the final state lepton (usually a muon) exits the fiducial region are considered partially-contained ("PC") and treated separately [27] from fully contained ("FC") events.

Turning first to the total rate, two independent published analyses ("A" and "B") [28] for the sub-GeV events, and a separate analysis for multi-GeV events [25], give

$$= 0.61 \pm 0.03(\mathrm{stat.}) \pm 0.05(\mathrm{syst.}), \quad \mathrm{sub-Gev, A} \tag{15}$$

$$R_{\mathrm{Data/MC}} = 0.65 \pm 0.03(\mathrm{stat.}) \pm 0.05(\mathrm{syst.}), \quad \mathrm{sub-GeV, B} \tag{16}$$

$$= 0.65 \pm 0.05(\mathrm{stat.}) \pm 0.08(\mathrm{syst.}), \quad \mathrm{multi-GeV} \tag{17}$$

The most recent results [29] combining FC and PC muons are

$$R_{\mathrm{Data/MC}} = 0.67 \pm 0.02 \pm 0.05\ , \mathrm{sub-GeV} \tag{18}$$

$$= 0.66 \pm 0.04 \pm 0.08\ , \mathrm{multi-GeV} \tag{19}$$

Rate Analysis			Zenith Angle Analysis		
Analysis A	Data	Monte Carlo	sub-GeV	Data	Monte Carlo
single-ring	1883	2030.5	single-ring	2389	2622.6
e-like	983	821.2	e-like	1231	1049.1
μ-like	900	1218.3	μ-like	1158	1573.6
multi-ring	784	759.2	multi-ring	911	980.7
total	2579	2789.7	total	3300	3603.3
$R = 0.61 \pm 0.03 \pm 0.05$					
Analysis B	Data	Monte Carlo	multi-GeV	Data	Monte Carlo
single-ring	2008	2185	single-ring	520	531.7
e-like	967	812.1	e-like	290	236
μ-like	1041	1364.8	μ-like	230	295.7
multi-ring	642	631.3	multi-ring	533	560.1
total	2650	2817.2	total	1053	1091.8
$R = 0.65 \pm 0.03 \pm 0.05$					
			PC	301	371.6

Table 1: Numbers of events used in rate and zenith angle analyses. Left panel are number of events of various types used in two separate rate analyses from [28]. Right panel are the event categories used in the zenith angle analysis [25].

The dominant uncertainty in each analysis comes from the calculation of the ν_μ/ν_e flux ratio (5%) and the neutrino charged current and neutral current cross sections (3-3.5% each). The shape of the momentum distribution of the final state lepton in single-ring events agrees with the Monte Carlo expectation, hence $R_{\rm Data/MC}$ appears to be independent of energy.

Combining the statistical and systematic errors in quadrature gives

$$R_{\rm Data/MC} \;<\; 0.78 \;\text{ at 95\% c.l.} \tag{20}$$

The average neutrino flight path is 6000 km, which gives

$$\delta M^2 \;>\; 2\times 10^{-4}\text{eV}^2 \;\text{ at 95\% c.l.} \tag{21}$$

Since the number of oscillations depends on neutrino flight distance, $R_{\rm Data/MC}$ should vary with the zenith angle. So too should the ν_μ event rate and/or the ν_e event rate out of which $R_{\rm Data/MC}$ is formed. The direction of the final state lepton approximates the neutrino flight direction within 55° at p_l=400 MeV/c and 20° at p_l=1 GeV/c. The path length is a very strong function of zenith angle: the average flight length for neutrinos produced above the horizon ($\cos\theta_Z > 0$) is 74 km while the path length for those produced below the horizon ($\cos\theta_Z < 0$) is 6500 km. As previously argued, in the absence of oscillation the detected flux of multi-GeV neutrinos is expected to be up-down symmetric, and detailed calculations indicate that any asymmetry should be less than a few percent.

Let $A = (U-D)/(U+D)$ be the asymmetry between the number of upward-going ($\cos\theta_Z < -0.2$) muons, U, and the number of downward-going ($\cos\theta_Z > 0.2$) ones, D. From the data in Table 1, published in [25],

$$A \;=\; -0.296 \pm 0.048 \pm 0.01 \;\; \text{multi}-\text{GeV, FC}+\text{PC}\;\mu \tag{22}$$

The updated result is [29]

$$A \;=\; -0.311 \pm 0.043 \pm 0.01 \;\; \text{multi} - \text{GeV}, \;\; \text{FC} + \text{PC}\; \mu. \tag{23}$$

In both cases, the asymmetry for electron events is consistent with zero.

The nonzero asymmetry for neutrino induced muon events clearly indicates something is happening: muon neutrinos are being lost as they transit the earth. The detailed zenith angle distribution is well fit by the hypothesis that the disappearing muon neutrinos are undergoing two-flavor oscillation into tau or perhaps sterile neutrinos.[2] Assuming $\nu_\mu \to \nu_\tau$, the favored values of the oscillation parameters are

$$5 \times 10^{-4} \;<\; \delta M^2 \;<\; 6 \times 10^{-3} \text{eV}^2 \;\; \text{and} \;\; \sin^2 2\theta > 0.86 \tag{24}$$

from the published analysis. For the updated results, with maximum mixing, which is favored, the 95% c.l. interval for δM^2 is

$$1.5 \times 10^{-3} \;<\; \delta M^2 \;<\; 6 \times 10^{-3}\ \text{eV}^2\ . \tag{25}$$

The allowed oscillation region is shown in Figure 5.

Neutrino decay has been considered as a mechanism to account for the loss of muon neutrinos traveling through the earth [18]. Although neutrino decay can account for the missing ν_μ flux, neutrino decay in vacuum does not account for the energy dependence of the zenith angle distribution observed experimentally. Including the effects of neutrino decay in matter improves the agreement somewhat, but leads to an underestimate on the number of upward going muon events [30].

4.1.2 Comments on the Results

At this point, it is useful to consider the numbers of events involved. Assuming the flux of electron neutrinos remains unchanged during transit through the earth, the number of observed e-like single ring events divided by the number expected gives a flux normalization of 1.17; the observed flux is 17% larger than predicted. Normalizing the number of expected single ring mu-like events by this factor gives an observed deficit of 550 mu-like events. Normalizing the number of multi-ring events in the same way gives a deficit of about 100 events, which is consistent with the number of ν_μ induced charged current events lost if $R_{\text{Data/MC}}$=0.6. For the zenith angle asymmetry, if $A = -0.3$, the number of upward ($\cos\theta_Z < -0.2$) mu-like single ring events, U, differs from the number of downward ($\cos\theta_Z > 0.2$) events, D, by $U - D \sim 110$ for the multi-GeV single ring sample and ~ 150 for the sub-GeV single ring sample. Thus, the conclusion that neutrinos oscillate rests on the deficit of a few hundred events in the flux ratio measurement, and about one hundred in the zenith angle measurement.

Taking a critical view, several ideas come to mind. Most obviously, misidentification of cosmic rays could increase the number of downward going muons which, when combined with the 20% absolute normalization uncertainty, could give the observed asymmetry. The angular resolution on the incoming neutrino

[2] Reactor neutrino oscillation experiments (see Section 6.1) probe the $1.5 \times 10^{-3} < \delta M^2 < 6 \times 10^{-3}$ eV^2 region using $\overline{\nu}_e$ disappearance, which is not observed. By CPT conservation, $\overline{\nu}_e \not\to \overline{\nu}_\mu \;\Rightarrow\; \nu_\mu \not\to \nu_e$, and therefore the reactor experiments rule out $\nu_\mu \to \nu_e$ oscillations as the origin of the deficit of atmospheric muon neutrinos.

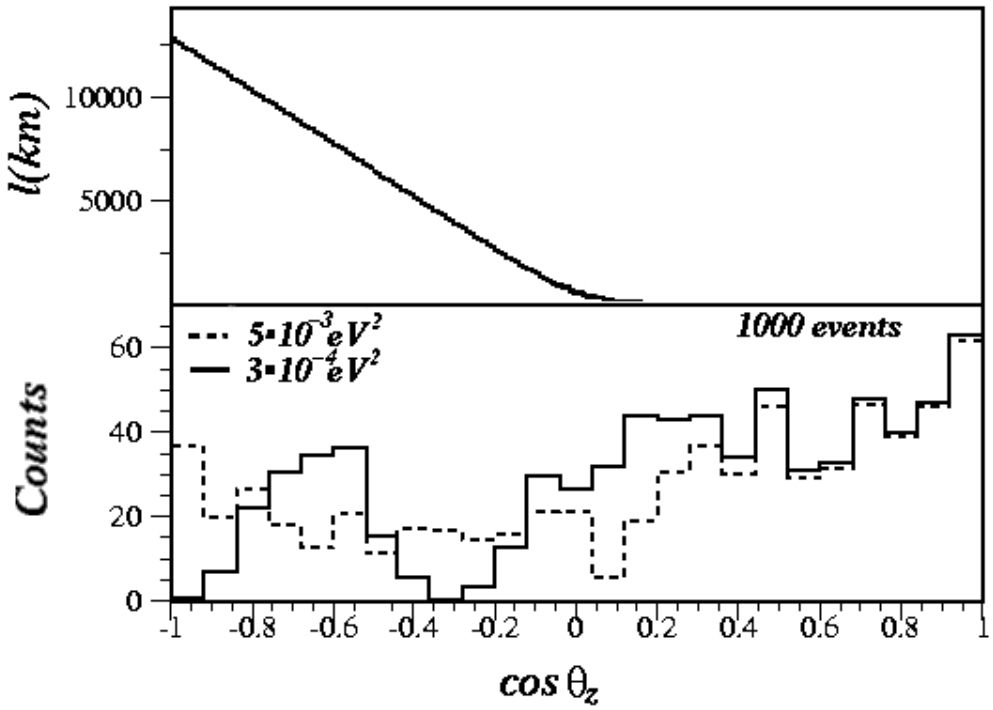

Figure 2: Zenith angle measurement. a) shows relation between $\cos\theta_Z$ and distance between production point and detector, b) shows the number of counts as a function of $\cos\theta_Z$ for selected δM^2 and maximal mixing with no angular smearing assuming 1 GeV atmospheric neutrinos. At 1 GeV, the SuperKamiokande angular resolution is 20^o.

direction (which arises primarily owing to the approximation of the incoming neutrino direction by the direction of the recoil lepton) largely washes out the oscillation signal and the measurement really amounts to a two bin ($\cos\theta_Z > 0.2$ and $\cos\theta_Z < -0.2$) measurement, as clarified by Figure 2. The effect could then be caused by an underestimate of the amount of background from downward going cosmic ray muons. Given that 10^8 cosmic ray muons traverse the detector each year, even a very small error in the veto efficiency would lead to a large asymmetry. However, Superkamiokande's outer detector acts independently of the inner detector, allowing independent veto calibration of the two systems. In addition, no systematic variation of A is observed when the vertex cut is relaxed to allow events closer to the surface of the inner detector [28]. The claim of complete absence of cosmic ray background in the final sample seems compelling.

Geomagnetic effects could also play a large role, especially for neutrinos with $E_\nu < 1$ GeV which would originate from lower energy primary particles. The earth's magnetic field bends cosmic ray primaries below a few GeV away from the earth near the equator where the component of the magnetic field perpendicular to the direction of travel of the cosmic rays is largest (~ 0.3G). Near the magnetic poles, the perpendicular component goes to zero, allowing cosmic rays of all energies to interact in the atmosphere. Downward going neutrinos originate from interactions which take place at latitude 40^oN, while upward going neutrinos originate from essentially all latitudes. One would suspect this would lead to the

Experiment	Exposure (kt-y)	$R_{\mathrm{Data/MC}}$
Soudan-2[33]	3.9	$0.66 \pm 0.11^{+0.05}_{-0.06}$
IMB-3[34]	3.4	0.80 ± 0.10
NUSEX[19]	0.74	$0.96^{+0.32}_{-0.28}$
Kamiokande[35]	7.7	$0.60^{+0.06}_{-0.05} \pm 0.05$ sub-GeV
		$0.57^{+0.08}_{-0.07} \pm 0.07$ multi-GeV
Frejus[22]	1.56	0.95 ± 0.18

Table 2: Summary of measurements of flavor composition of atmospheric neutrinos from underground experiments.

downward going neutrinos having a harder energy spectrum owing to the harder spectrum of the primaries. Calculation reveals the size of the effect has only a 1-2% impact on A [31] for the multi-GeV sample, much too small to account for the observed asymmetry. In addition, SuperKamiokande has measured the azimuthal (or "East-West") distribution of neutrino events from near the horizon[32] and observes the geomagnetic asymmetry predicted by [31].

Atmospheric neutrinos were extensively studied by the other large underground experiments. Almost all observe a deficit of μ-like events leading to a low value for $R_{\mathrm{Data/MC}}$, Table 2. Particularly significant in these results is the confirmation of this anomaly in both major types of detectors, water Čerenkov (Kamiokande, IMB-3 and Superkamiokande) and dense sampling detectors (Soudan-2).

4.1.3 Upward Going Muons

Measurement of the flux of upward going muons also provides information about atmospheric neutrino oscillations. Neutrino interactions in the rock surrounding the detector produce muons energetic enough (energies above a few GeV) to pass through the detector. The direction of the scattered lepton roughly approximates the neutrino direction. However, since only muons are detected, the extraction of an oscillation signal relies on the calculation of the normalization and angular distribution of the flux via Monte Carlo and is thus more prone to systematic uncertainty.

SuperKamiokande [36] has measured a total of 614 upward through going muons with energies above 1.6 GeV. The measured flux agrees with calculation within the (large) errors. The zenith angle distribution peaks more sharply at the horizon ($\cos\theta_Z \sim 0$) than expected for the no-oscillation case. The best fit gives $10^{-3} < \delta M^2 < 10^{-1}$ eV^2 for $\sin^2 2\theta > 0.4$. The flux is 14% lower than predicted in [16].

A measurement of the upward going muon flux by the MACRO experiment [37] also differs from the no oscillation expectation. MACRO, a 5 kiloton detector, uses streamer tubes and scintillator to measure the trajectory and velocity with 1 cm and 1 ns precision, respectively, allowing the measurement of upward through going muons produced by neutrinos with energies $E_\nu = 1 - 100$ GeV. A total of 451 ν induced events are measured (479 with a background of 28 ± 7) while 612 are expected and, as with SuperKamiokande, the zenith angle distribution peaks somewhat more at the horizon. A fit to the zenith angle distribution gives

$2 \times 10^{-4} < \delta M^2 < 2 \times 10^{-2}$ eV^2 for $\sin^2 2\theta > 0.5$.

4.1.4 Summary

In summary, a deficit of ν_μ induced events appears in almost all of the measurements, the most precise of which comes from SuperKamiokande. In addition, SuperKamiokande measures a zenith angle dependent ν_μ flux which, although statistically less significant, is less prone to theoretical uncertainty than the flux measurement. The data are well fit by the hypothesis of neutrino oscillation. The measurement of the upward going muon flux and the agreement between the predicted and measured azimuthal ν_μ induced event asymmetry provide important supporting evidence in favor of this hypothesis.

4.2 Solar Neutrinos

The sun produces electron neutrinos via nine principal reactions in the *pp* chain, starting with the fusion of two protons to make a deuteron and ending with the production of ^{4}He [38]. The neutrino energies range from 0 to 15 MeV and three of the fusion reactions result in mono-energetic ν_e's at 380, 860 and 1400 keV, Figure 3. The calculation of the solar neutrino flux [39] has an uncertainty of less than 3%, and therefore one can probe for neutrino oscillation by searching for ν_e disappearance.

4.2.1 Experiments and Results

Three different types of experiments have measured the solar neutrino flux. Owing to the different experimental techniques, each measures a different portion of the neutrino energy spectrum. Water Čerenkov [41, 24, 42, 43] counters detect neutrinos via $\nu_e + e^- \rightarrow \nu_e + e^-$ and, owing to their relatively high energy threshold of 5-7 MeV, detect only the upper part of the ^{8}B ν_e spectrum. The original solar neutrino experiment [44] relies on the reaction $\nu_e + ^{37}\mathrm{Cl} \rightarrow ^{37}\mathrm{Ar} + e^-$ in perchloroethylene, which has a threshold of 814 keV, giving sensitivity to the ^{8}B, ^{7}Be, and *pep* neutrinos and the upper part of the CNO spectrum. Finally, the SAGE [45] and Gallex [46] experiments use the capture reaction $\nu_e + ^{71}\mathrm{Ga} \rightarrow ^{71}\mathrm{Ge} + e^-$ in metallic gallium (SAGE) or gallium chloride (Gallex) with a threshold of 232 keV. This provides a window for detection of the *pp* ν_es. The fluxes observed by the various experiments are compared in Table 3 with the values predicted assuming that neutrinos do not oscillate.

These experiments have very different systematic effects. The $\nu_e + e^- \rightarrow \nu_e + e^-$ elastic scattering used by the water Čerenkov experiments gives a correlation (within about 25°) between the recoil electron and the incident neutrino direction, allowing the rejection of the isotropic backgrounds from the gamma ray photons emitted by radio-contaminants in the detector itself. Decay products from ^{16}O created by spallation reactions induced by cosmic ray muons are also a serious background and are rejected via time and spatial correlation with the track from the cosmic ray muon entering the detector. The clear correlation between the sun's location and the incident neutrinos (see [42], Figure 2) gives a large measure of comfort that the observed events are the result of stellar processes.

The other three experiments rely on the exposure of a large target mass to the ν_e from the sun, which convert a few atoms per day in the target to a radioactive

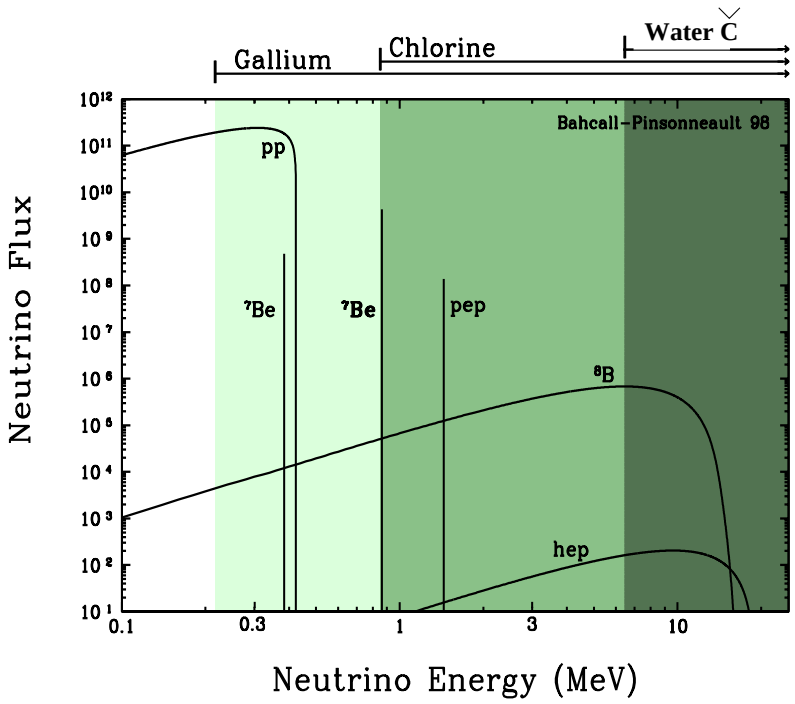

Figure 3: Energy spectrum at earth of solar neutrinos. The flux for lines is given as neutrinos cm^{-2}-s. The continuous spectra are in units of neutrino cm^{-2}/MeV/s. From [40].

daughter (via induced beta decay), which is then removed from the target mass chemically and detected via the x-ray from electron capture induced decay. For both the chlorine and gallium experiments, the daughter nucleus was extracted as a gas and detected in proportional counters via the subsequent electron capture decay. The collection efficiency is close to 100% and detection efficiency around 50%. Background enters primarily through the counting procedure where cosmic ray muons and gammas from radio-isotope contamination (primarily from airborne radon) contribute about 10% to the overall counting rate. While the nature of the experiments does not allow direct verification that the neutrinos actually come from the sun, both gallium experiments performed calibrations using a ^{51}Cr [47] source which provided 751 keV ν_e via $e^- + {}^{51}\mathrm{Cr} \rightarrow {}^{51}\mathrm{V} + \nu_e$. In both cases the calibration confirmed the expected collection and counting efficiencies, with $R_{calib/calc} = 83 \pm 10\%$ for Gallex and $95 \pm 11^{+5}_{-8}$ for SAGE.

The original observation of solar neutrinos was made by the Homestake experiment [44], which has been in operation almost continuously since 1970. The target consists of 615 metric tons of C_2Cl_4, which provides about 2×10^{30} target ^{37}Cl atoms. Solar neutrinos with energies above 814 keV are absorbed via the reaction $\nu_e + {}^{37}\mathrm{Cl} \rightarrow {}^{37}\mathrm{Ar} + e^-$ to give ^{37}Ar which decay via electron capture with a half-life of 35 days. The measurement is performed as a series of exposures of four to six weeks during which time the concentration of ^{37}Ar builds up to saturation. The ^{37}Ar is then extracted by bubbling helium through the tank and chemically separating the ^{37}Ar into a proportional tube where the number of ^{37}Ar atoms are counted via the detection of the Auger electron from their electron capture

Target	Experiments	Observed/Expected Rate	Source
^{37}Cl	Homestake	$0.331\ ^{+0.061}_{-0.053}$	^{8}B,^{7}Be
^{71}Ga	SAGE	$0.519\ ^{+0.070}_{-0.066}$	$pp, pep,^{7}$Be
	Gallex	$0.605\ ^{+0.060}_{-0.054}$	
H_20	SuperKamiokande	$0.470\ ^{+0.061}_{-0.054}$	^{8}B
	Kamiokande	$0.56\ ^{+0.091}_{-0.054}$	

Table 3: Results from solar neutrino experiments. Expected fluxes are from [48].

decay.

In addition to a measurement of the total flux of solar neutrinos above 5.5 MeV, SuperKamiokande [43] has measured the recoil energy spectrum of electrons above 5.5 MeV, which gives an indication of the energy spectrum of solar neutrinos. The energy scale is calibrated to a precision of 0.8% at 10 MeV using a combination of a dedicated LINAC, ^{16}N (from muon spallation) and muon decay. The resulting spectrum is harder than expected even for the MSW oscillation result favored by the total rate measurements. An earlier, much less precise measurement [24] showed no disagreement with the expected flux.

SuperKamiokande has also measured the variation of the solar neutrino flux depending on whether the neutrinos from the sun pass through the earth or not (the "day/night" effect)[49]. Day/night variation could be caused by MSW oscillations in the earth. The measured flux ratio is

$$\frac{\Phi_{night}}{\Phi_{day}} = 1 + 0.047 \pm 0.042(\text{stat.}) \pm 0.008(\text{syst.}) \tag{26}$$

indicating no day/night effect at the 10% level.

4.2.2 Combined Analysis and Future Probes

Several combined analyses of all the solar neutrino data have been carried out [39, 48]. Perhaps the most impressive allows normalizations of the *pp*, ^{7}Be, ^{8}B and CNO neutrino spectra to vary while assuming that neutrinos do not oscillate. No combination of normalizations reproduces the observations with significant compatibility, indicating that some new phenomenon, consistent with neutrino oscillations, takes place regardless of the details of the solar model. If one assumes that solar neutrinos do undergo oscillations, either of the MSW variety within the sun, or of the vacuum variety between the sun and the earth, then a good fit to all the solar neutrino data, apart from the new data on the energy spectrum, can be obtained. The best fit global solutions are summarized in Table 4. Inclusion of the limit on the day/night variation tends to push the lower limit on δM^2 to above 10^{-5} eV^2 for the large-angle MSW solutions [49, 50].

All the results in Table 4 are in some contradiction with the SuperKamiokande recoil spectrum measurement, with the largest deviation being at the highest electron recoil energies. It will be interesting to see how this situation evolves as the spectrum measurements become more precise.

Whether the electron neutrinos produced in the sun oscillate to active (ν_μ or ν_τ) or sterile neutrinos will be largely resolved by the Sudbury Neutrino Observatory (SNO) [51] experiment, which will begin operation next year with a

Type	Large angle	Small angle
MSW $\nu_e \to \nu_{\text{Active}}$	$\delta M^2 = 1.8 \times 10^{-6}\text{eV}^2$ $\sin^2 2\theta = 0.76$	$\delta M^2 = 5.4 \times 10^{-6}\text{eV}^2$ $\sin^2 2\theta = 6.0 \times 10^{-3}$
MSW $\nu_e \to \nu_{\text{Sterile}}$		$\delta M^2 = 4.3 \times 10^{-6}\text{eV}^2$ $\sin^2 2\theta = 6.9 \times 10^{-3}$
Vacuum	$\delta M^2 = 8.0 \times 10^{-11}\text{eV}^2$ $\sin^2 2\theta = 0.75$	

Table 4: Best fit results to all solar neutrino flux data [39].

target of 1 kiloton of heavy water (D_2O). The use of a heavy water target allows the simultaneous measurement of the charged current and neutral current cross sections via

$$\nu_e + d \rightarrow p + p + e^-(\text{CC}) \tag{27}$$

$$\nu_x + d \rightarrow p + n + \nu_x(\text{NC}), \tag{28}$$

where ν_x refers to ν_e, ν_μ or ν_τ. The first reaction will measure the flux of solar ν_e, while the second reaction will measure the total flux of ν_e, ν_μ and ν_τ. If the MSW effect or vacuum oscillation converts solar electron neutrinos into sterile neutrinos, the rate for the second reaction will be lower than if the conversion is to active neutrinos. The SNO experiment will be sensitive only to ^{8}B neutrinos. The rates expected assuming 50% of the solar neutrinos oscillate are 5.5 NC events per day (assuming 40% detection efficiency) and 12.7 CC events per day. Thus, the experiment should resolve the situation after two years of operation. The heavy water target is surrounded by a 7800 ton pure water buffer and is viewed by 9456 photo-multiplier tubes. The Čerenkov ring from each final state charged particle gives its direction, and the number of Čerenkov photons gives the particle's total energy. The neutrons produced in the neutral current scattering are detected by delayed coincidence; they first thermalize in the target and are subsequently captured on a proton, giving a 2.2 MeV gamma ray.

In the coming years, SNO, SuperKamiokande and BOREXINO will make important inroads in the measurement of the solar neutrino energy spectrum. In particular, BOREXINO [52], located in the Gran Sasso, will measure the ^{7}Be neutrino flux using $\nu_e + e^- \to \nu_e + e^-$. The detector consists of 300 tons of very high radio-purity scintillator (less than 10^{-14} g of U, Th and Rn per gram of scintillator) viewed by 2000 photo-multiplier tubes. The arrival time of the scintillation photons at the PMT will be used to locate the event vertex inside a 100 ton fiducial volume and the total signal from all PMTs will give the energy of the recoil electron. BOREXINO plans to achieve a 250 keV threshold, which will allow the detection of ^{7}Be ν_e which will create recoil electrons up to 660 keV. For the standard solar model with no oscillations, the count rate is expected to be 55 events per day. If the MSW effect is operative, the count rate would be reduced, and its value may discriminate between the large and small angle MSW solutions. In addition, the high statistics of BOREXINO will allow the seasonal variation to be measured, which is expected to be large if vacuum oscillations are taking place.

The next few years should see a resolution of the solar neutrino problem: we can expect measurements of the ν_e energy spectrum at several points which will

distinguish between the small- and large-angle MSW possibilities. Measurements of the seasonal variation will determine if vacuum oscillations are taking place. Finally, comparison of the neutral and charged current rates will clarify the role of sterile neutrinos.

4.3 The LSND Experiment

To date there are only two claimed positive observations of neutrino oscillations from an accelerator-based neutrino source, both from the LSND (Liquid Scintillator Neutrino Detector) experiment at the LAMPF neutrino source. LSND has not only the sole observation of oscillations from human-made neutrinos, but also the only appearance signal among our three hints of oscillations. The LAMPF accelerator produces a large current of nearly relativistic protons, and a large number of π^+ are produced in a long water target upstream of a copper beam stop. Most of these protons come to rest and then decay *via* the familiar chain, $\pi^+ \to \mu^+\nu_\mu$, $\mu^+ \to e^+\nu_e\overline{\nu}_\mu$, where the muon decays at rest. The charge conjugate chain beginning from π^- is suppressed by approximately three orders of magnitude, roughly one each from production, absorption of π^- in the beam stop, and atomic capture of μ^- before decay [53]. Therefore, a $\overline{\nu}_e$ appearance signal is relatively free of beam-induced backgrounds. LSND also searches for the appearance of high-energy ν_e (above the endpoint of $\mu^+ \to e^+\overline{\nu}_\mu\nu_e$ decay at rest), which could result from $\pi^+ \to \nu_\mu\mu^+$ in flight, and $\nu_\mu \to \nu_e$ [54]. The experiment observes significant excesses of both $\overline{\nu}_e$ and ν_e, which it attributes to $\overline{\nu}_\mu \to \overline{\nu}_e$ from muon decay at rest and $\nu_\mu \to \nu_e$ oscillations from pion decay in flight, respectively. The $\overline{\nu}_e$ appearance signal is more significant than the ν_e signal because of higher statistics, and lower beam-related and detector-related backgrounds.

The two favored regions in the space of two generation oscillation parameters for the interpretation of these excesses are shown in Figure 4. The two favored regions in this space are consistent. After background subtraction, the mean energy of the excess $\overline{\nu}_e$ is roughly a factor of two lower than the mean energy of the excess ν_e, and thus the two appearance experiments are sensitive to different δM^2. The high δM^2 oscillation probabilities from $\overline{\nu}_\mu(\nu_\mu) \to \overline{\nu}_e(\nu_e)$ in the two analyses are presented as $(3.1^{+1.1}_{-1.0} \pm 0.5) \times 10^{-3}$ and $(2.6 \pm 1.0 \pm 0.5) \times 10^{-3}$, respectively. The ν_e analysis observes an excess with a somewhat harder energy spectrum than ν_μ oscillations might predict and therefore weakly favors high δM^2. The $\overline{\nu}_e$ analysis strongly favors low δM^2.

On the face of it, LSND's statistical evidence, at least for the $\overline{\nu}_e$ appearance observation, is overwhelming. Suggestions have been made that one portion of the $\overline{\nu}_e$ suppression in the π^- decay-at-rest chain could be significantly altered, by, for example, meta-stable π^--N bound states, but there appears to be no compelling case for proving such a hypothesis. Another alternative to an oscillation explanation is the production of unexpected $\overline{\nu}_e$ in the LSND decay chain *via* lepton-flavor violating processes in left-right symmetric models, in R-parity violating SUSY and in model-independent frameworks [55]. Such processes are strongly constrained by existing data on rare muon decays and on muonium-antimuonium conversion, and do not appear to yield a convincing non-oscillation explanation at this time.

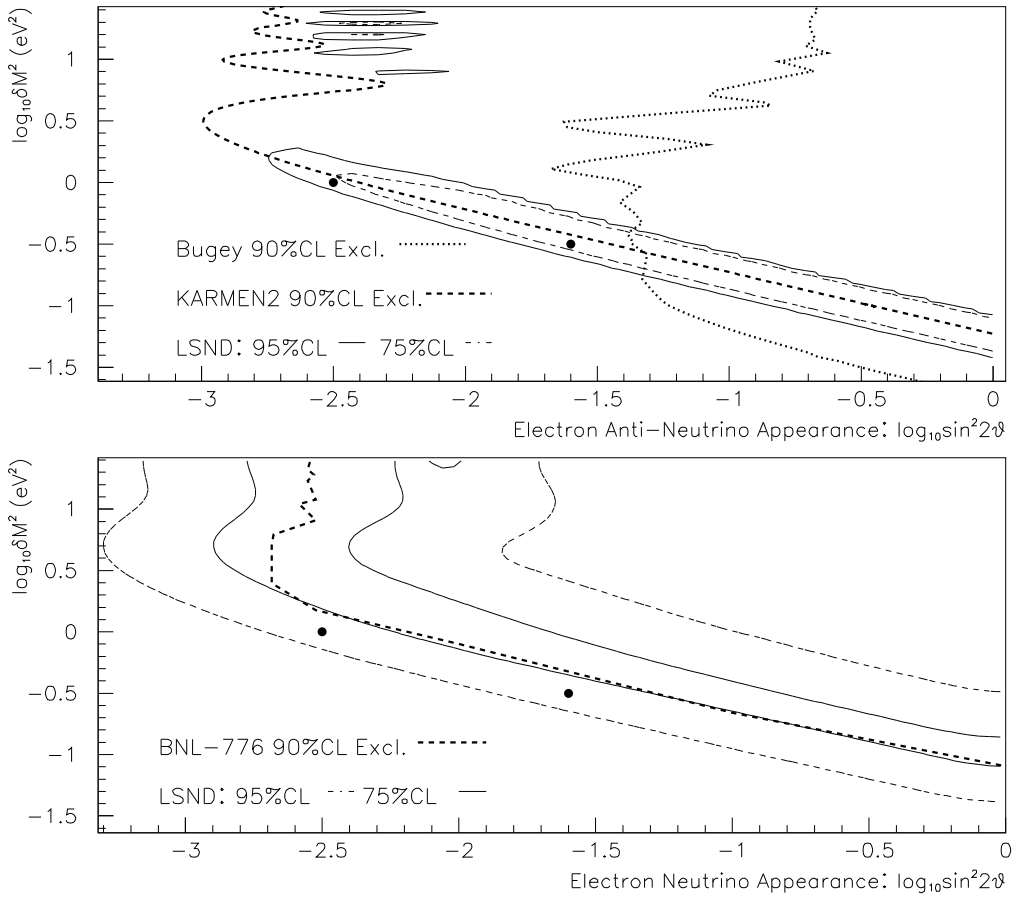

Figure 4: The 95% C.L. regions for $\overline{\nu}_\mu \to \overline{\nu}_e$ and $\nu_\mu \to \nu_e$ oscillations from the LSND $\overline{\nu}_e$ and ν_e excesses. *(Data provided courtesy of the LSND collaboration.)* Shown also are the 90% C.L. exclusion curves for the ongoing KARMEN2 experiment *(preliminary limit provided by courtesy of R. Maschuw)* as of January 1999, for the Bugey reactor experiment, and for BNL-E776. Higher δM^2 are ruled out by CCFR, NOMAD and NuTeV data. Two points in the LSND-favored region from the $\overline{\nu}_e$ appearance analysis are shown to guide the eye.

4.3.1 LSND AND COMPETING NULL RESULTS

While LSND is the only accelerator experiment to observe oscillations to date, many other experiments have probed oscillations in regions of the favored LSND oscillation parameter space. These competing experiments can be grouped into three categories: experiments with a similar beam and energy range (KARMEN and KARMEN2), reactor experiments and high-energy experiments.

The KARMEN and KARMEN2 experiments at the ISIS neutron spallation facility use a beam, like the LSND beam, produced primarily from pion decay and muon decay at rest. However, the 100 ns pulsed KARMEN beam has a very low duty cycle ($\sim 10^{-5}$) and allows for time-based separation of π^+ and μ^+ decay products. The KARMEN experiment had a significant background from neutrons produced in the shielding which limited its sensitivity; however, the KARMEN2 upgrade has reduced this background enormously [56].

Based on a nearly 3000 Coulomb exposure, KARMEN2 initially reported a signal of 0 ν_e candidate events where a background of 2.88 ± 0.13 events was expected [56]. However, an updated analysis based on nearly 4000 Coulombs with looser cuts now reports 7 observed events with an expected background of 9.3 events [57]. Despite seeing no signal, KARMEN2 currently lacks the sensitivity to convincingly rule out the LSND observation. However, should KARMEN2 improve its sensitivity and continue to see no evidence of oscillation into $\overline{\nu}_e$, it may call into question the reproducibility of the LSND $\overline{\nu}_e$ excess, since the beams and detection mechanisms are so similar.

Reactor experiments, which are discussed in more detail in Section 6.1, are disappearance experiments at low neutrino energy and are therefore sensitive to high $\sin^2 2\theta$ and low δM^2. The observation of no oscillation signal from the Bugey experiment in the $\overline{\nu}_e \to \overline{\nu}_e$ channel limits the possible $\overline{\nu}_\mu \to \overline{\nu}_e$ probability, and therefore excludes the LSND favored region at high mixing angle.

High-energy accelerator experiments currently suffer from generally insufficient L/E to probe the LSND δM^2 "knee" in Figure 4. Most accelerator experiments also probe primarily $\nu_\mu \to \nu_e$, although the NuTeV experiment expects to be sensitive to the LSND region above δM^2 of ~ 20 eV^2 in its $\overline{\nu}_\mu$ beam [58]. CCFR [59] and NOMAD [60] rule out the LSND favored region above 25 and 10 eV^2, respectively, and the result from BNL-E734 [61] rules out much of the LSND favored oscillation parameters in the same δM^2 region. BNL-E776, with its sensitivity to larger L/E comes the closest of any existing experiment to overlapping the LSND favored region [62]. Like KARMEN2, BNL-E776 cannot probe the entire LSND favored region in the $\overline{\nu}_e$ signal at lowest δM^2. However, the BNL-E776 result does exclude the most probable values from the LSND decay-in-flight analysis, as shown in Figure 4.

4.3.2 FUTURE TESTS OF THE LSND RESULT

Future accelerator experiments are planned to search for oscillations in the LSND favored region. An experiment, BooNE [63], has been approved for single-detector operation at Fermilab, and an experiment at CERN with a similar baseline and beam energy, I-216 [64], is also being proposed. Both experiments hope ultimately to use neutrino beams of about 1 GeV to study ν_e appearance in detectors at two different values of L. Because of the energy regime, both experiments expect large detector and beam backgrounds to ν_e appearance; however, this next generation

of experiments should have the raw statistical power to convincingly address the entire LSND favored region.

5 A COSMOLOGICAL CONSTRAINT ON NEUTRINO MASS

We now turn from the positive hints of neutrino mass to a discussion of the constraints on this mass from cosmology and from negative laboratory searches.

Owing to the great abundance of neutrinos in the universe, even tiny neutrino masses can lead to a significant neutrino contribution to the mass density of the universe. As a result, our information on this mass density provides a fairly stringent upper bound on neutrino mass.

Increasing evidence from several sources suggests that [65, 66]

$$\Omega_M = 0.1 - 0.4 \ , \tag{29}$$

where Ω_M is the total mass density of the universe, as a fraction of the critical density required to stop indefinite expansion. This Ω_M includes a contribution from baryons. Very likely, it also includes a contribution from non-baryonic Cold Dark Matter (CDM) particles, which are much heavier than neutrinos. These heavier particles appear to be needed to help seed the early-universe formation of the observed galactic structure. Finally, Ω_M may include a contribution from Hot Dark Matter (HDM) particles. These are long-lived particles with masses much less than 1 keV, which would have been relativistic at the early time important for galactic structure formation. If neutrinos are massive, their contribution to Ω_M, Ω_ν, is a part of the HDM contribution.

The HDM part of the mass density cannot be too large, because in the early universe any HDM would have acted as a drag interfering with the formation of the observed galactic structure. From this fact, the bound $\Omega_M \lesssim 0.4$ (Eq. (29)), and the fact that some of Ω_M comes from baryons and from non-baryonic CDM, one may conclude conservatively [66] that the HDM part of Ω_M does not exceed 0.2. This means that, in particular, $\Omega_\nu \lesssim 0.2$.

For any neutrino mass eigenstate ν_m which is a constituent of active flavor neutrinos, the present number density in the universe is fixed at 115/cc by thermal equilibrium in an early era [67]. Thus, if ν_m has mass M_m, its present mass density is 115 M_m/cc. Now, the present critical density is $1.05 \times 10^4 h^2$ eV/cc, where h is the Hubble constant in units of 100 km/sec/Mpc. Hence, assuming $h \simeq 0.65$, the contribution of ν_m to Ω_ν is $M_m/40$ eV. If ν_e, ν_μ, and ν_τ are made up out of three mass eigenstates with masses M_1, M_2, and M_3, these mass eigenstates together yield

$$\Omega_\nu = (M_1 + M_2 + M_3)/40 \text{ eV} \ . \tag{30}$$

Requiring that $\Omega_\nu \lesssim 0.2$, we obtain the cosmological upper bound on neutrino mass

$$M_1 + M_2 + M_3 \lesssim 8 \text{ eV} \ . \tag{31}$$

6 NEGATIVE SEARCHES FOR NEUTRINO MASS

6.1 Reactor Oscillation Searches

Nuclear power reactors have always played a central role in neutrino physics. Neutrinos were first observed at a reactor [68] using

$$\overline{\nu}_e + p \rightarrow n + e^+. \tag{32}$$

The positron is detected via its ionization energy followed by detection of the Compton scattering of the two 511 keV gammas from the annihilation with an electron at rest. The neutron thermalizes and is then captured by a stable isotope (in this case cadmium) with a high capture cross section to form a gamma emitter whose gammas are then detected. This gives a double delayed coincidence which provides a powerful means for background rejection. Reactors emit $8 \times 10^{20}\nu$/s per gigawatt (electrical) power, so a one ton target mass 100 meters from a reactor core will detect a few neutrino events per hour. The neutrinos emitted by the reactor have an average energy of 3 MeV, so this type of experiment allows the probing of the $\delta M^2 \sim 10^{-2}$ eV^2 region. Owing to the low neutrino energy, only $\overline{\nu}_e$ disappearance experiments are possible, restricting the sensitivity to the mixing angle to $\sin^2 2\theta > 0.1$.

Two first generation reactor neutrino oscillation experiments probed the $\delta M^2 \sim 10^{-2}$eV^2 range [69]. Both were one ton target masses at $L = 100$m and used ^{3}He filled wire chambers to detect the neutron, giving efficiencies of around 15-20%. In both experiments, data was taken at different distances from the reactor, allowing two different measurements. The first was the comparison of the positron energy spectrum between different distances; the oscillation pattern depends on L/E, so changing L would change the neutrino energy spectrum and thence the positron energy spectrum. This allowed the measurement to be performed with no *a priori* knowledge of the neutrino energy spectrum from the reactor. In the second analysis, the knowledge of the fuel composition in the reactor core was used to calculate the expected flux which could then be used to compute the expected positron energy spectrum at a given distance. Different calculations of the flux were found to agree at the 3% level with dedicated measurements [70], removing the necessity of moving the detectors in future, larger experiments.

The current generation of reactor oscillation experiments, Chooz [71] and Palo Verde [72], have target masses of several tons (5 t and 12 t, respectively) and are located roughly 1 km (0.74 km and 1 km, respectively) from the several reactors. Both use liquid scintillator targets loaded with 0.1% Gd (by weight), which has a high neutron capture cross section and which radiates 8 MeV of gamma rays after capture. This detection scheme gives a significantly higher detection efficiency for the neutrons, resulting in higher performance overall.

Both experiments report null results and rule out $\overline{\nu}_e \rightarrow \overline{\nu}_x$ oscillations for $\delta M^2 > 9\times10^{-4}$eV^2 and $\sin^2 2\theta > 0.1$, Figure 5. Combined with the atmospheric neutrino measurements from SuperKamkiokande, the reactor measurements indicate that at the 90% confidence level, the atmospheric ν_μ oscillate into ν_τ or a sterile neutrino, rather than into ν_e. Both reactor experiments are continuing to run and will eventually reach $\delta M^2 \sim 10^{-4}$eV^2 for large mixing angles. If no oscillation effect emerges, they will completely exclude $\nu_\mu \rightarrow \nu_e$ as the primary oscillation process observed by SuperKamiokande.

A very ambitious experiment, KAMLAND [73], seeks to use the old Kamiokande site to situate a 1 kiloton detector 150 km from a complex of several reactors, giving a sensitivity of $\delta M^2 \sim 2\times10^{-5}$ eV^2. As KAMLAND is a disappearance ex-

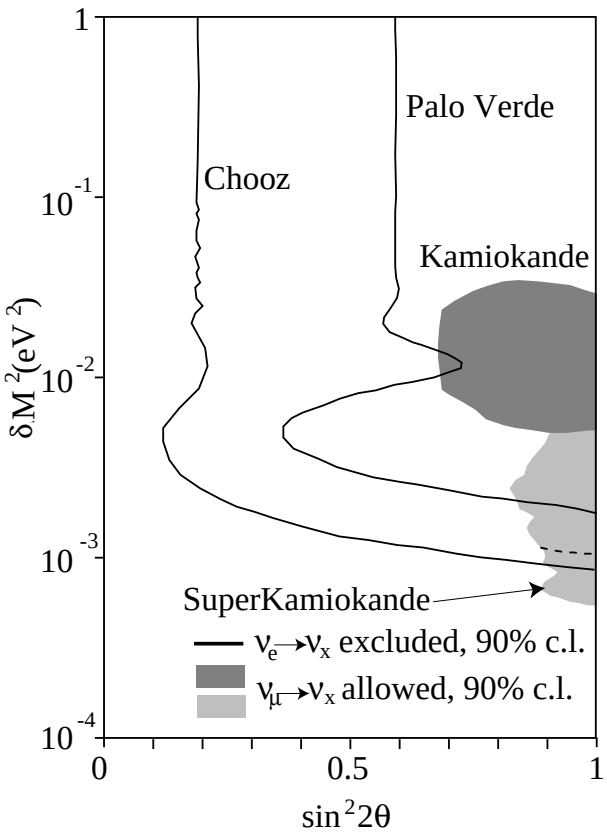

Figure 5: Exclusion plot for reactor neutrino experiments. Also shown is the allowed region from the atmospheric experiments. The dotted line in the SuperKamiokande region indicates a lower bound on δM^2 obtained from Ref. [36], an analysis of upward-going muon data.

periment, it would only be sensitive to $\sin^2 2\theta > 0.1$ and would effectively resolve between the large and small angle MSW solutions to the solar neutrino measurements. KAMLAND would use a large scintillator target viewed by roughly 2000 phototubes, giving a signal rate of two events per day. It is thought that through careful selection of construction materials and purification of the scintillator target, the background rate could be reduced to 0.1 events per day. KAMLAND is planning to take data for three years starting in 2001.

The scattering of reactor neutrinos from electrons at low energies may be used to measure the neutrino magnetic moment μ_ν. In the standard model, $\mu_\nu \sim 10^{-19} M_\nu(\text{eV})\ \mu_\text{B}$ for Dirac neutrinos and $\mu_\nu = 0$ for Majorana neutrinos; in both cases too small to explain any of observed oscillation effects. The current laboratory limit is $\mu_\nu < 10^{-10}\mu_B$ at 95% c.l. [74]. In the near future, the MUNU collaboration plans to use a 1 m^3 TPC with a recoil electron threshold near 100 keV to push the sensitivity to $3 \times 10^{-11}\mu_B$ [75].

6.2 Accelerator Oscillation Searches

Aside from the appearance signal at the LSND experiment that was discussed in Section 4.3, there is no other evidence for neutrino oscillations observed in accelerator-based experiments. Nevertheless, accelerator experiments are the preferred venue for studying neutrino oscillation phenomena because of the ability to control and vary L/E (and thus δM^2 sensitivity) in a neutrino beam and the ability to precisely determine flavor content of the neutrino beam at the point of creation. However, the practicalities of accelerator experiments place severe restrictions on our ability to probe the L/E regions favored by current non-accelerator observations of oscillation. In this Section, we summarize the current capabilities and status of accelerator experiments, as well as future expectations.

High intensity neutrino beams at accelerators are typically produced by high energy hadronic interactions in a fixed target which copiously produce forward secondary mesons, $\pi^\pm$ and $K^\pm$ in particular. These mesons can then be captured and focused parallel in electromagnetic beam optics, where the mesons are then allowed to decay weakly to a tertiary "beam" of neutrinos, predominantly ν_μ and $\overline{\nu}_\mu$. The efficiency for this process varies with the type of beam optics and primary beam energy, but 10^{-2}–10^{-5} neutrinos per incident hadron is a representative range. Because the neutrinos cannot be subsequently focused, at long distances L from the production point the neutrino flux varies with L^{-2}. Experiments may be roughly divided into two categories, short-baseline experiments which locate their detectors as close as possible to the point of neutrino production to maximize statistics, and long-baseline experiments which pick a longer L in order to tune L/E sensitivity to the desired range. Contemporary high energy neutrino beams optimized for statistics run at beam energies from a few GeV to a few hundred GeV, and shielding concerns require an L of 100 m–1 km, thus setting the "natural" range of δM^2 sensitivity at 10–100 eV^2. Lower δM^2 sensitivity, made interesting by the solar and atmospheric neutrino oscillation signals, requires longer L and/or lower E. Lower E allows the use of more intense primary beam sources to generate the beam, but decreases the neutrino cross-section (roughly proportional to $\sqrt{s}$) and increases the beam divergence (roughly proportional to γ^{-1}, the inverse Lorentz factor for the weakly-decaying parent particle). Charged-current production of τ leptons from nuclear targets has a neutrino energy threshold of $m_\tau + m_\tau^2/2m_N \sim 3.3$ GeV and suffers from

Experiment	$\langle E_\nu \rangle$	Baseline	Fiducial Mass	$\nu_\mu(\overline{\nu_\mu})$ CC/yr
CCFR/NuTeV	100 GeV	1 km	350 ton	10^6
CHORUS	30 GeV	0.6 km	0.8 ton	3×10^4
NOMAD	30 GeV	0.6 km	3 ton	10^5
MINOS	5–15 GeV	730 km	3.3 kton	10^4–3×10^3
K2K	2 GeV	250 km	22 kton	5×10^2
I-216	1.5 GeV	1 km	150 ton	5×10^4

Table 5: Approximate neutrino beam and detector parameters for a selection of current and near future accelerator-based neutrino oscillation experiments. The mean E_ν refers to observed neutrinos.

significant mass suppression until E is far above this threshold. Longer L results in an L^{-2} decrease in statistics as noted above. The argument has been made [76] that in a long-baseline appearance experiment the number of observed wrong-flavor neutrinos when $\delta M^2(\mathrm{eV}^2)L/E(\mathrm{km/GeV}) \ll 1$ is constant with L; however, it should be noted that backgrounds will not be constant with L and that an experiment with $\delta M^2 L/E \ll 1$ leaves no possibility to measure δM^2. Some neutrino beam and detector parameters for current and planned experiments are summarized in Table 5.

The most sensitive current results come from several generations of experiments with relatively short baselines, and therefore little sensitivity to the δM^2 of the three current neutrino oscillation observations. The most sensitive $\nu_\mu \to \nu_\tau$ searches to date come from the CHORUS and NOMAD experiments at CERN, which set upper limits in $\sin^2 2\theta$ of ~ 1–3×10^{-3} at their peak sensitivity around δM^2 of ~ 30 eV^2, and which exclude δM^2 above ~ 2 eV^2 at maximal mixing [77, 78]. Both experiments expect to improve their mixing angle limits significantly when all their data is analyzed. The most sensitive searches for $\nu_\mu \to \nu_e$ oscillation come from the CCFR/NuTeV [59], NOMAD [60], BNL-E734 [61] and BNL-E776 [62] experiments, and these results were discussed in Section 4.3 and displayed in Figure 4.

The next generation of oscillation experiments offers significant hope of probing the oscillations reported by the LSND and atmospheric neutrino experiments. Experiments targeted on the former (BooNE, I-216) were discussed in Section 4.3. The long-baseline experiments searching for evidence of the latter include MINOS at Fermilab-Soudan [79], K2K at KEK-Kamiokande [80], and ICARUS [81], NOE [82] and OPERA [83] at CERN-Gran Sasso. By virtue of their L/E ratio, each of these experiments has a peak sensitivity at $\delta M^2 \sim 10^{-2}$ eV^2. Their ν_τ appearance capabilities differ substantially, however. Most notably, by virtue of its low energy beam, K2K only has the possibility to detect ν_τ through neutral current interactions, such as $\nu_\tau N \to \nu_\tau \pi^0 X$.

Studies of CP violation in the atmospheric region of δM^2 are potentially interesting because an observed CP asymmetry would indicate that there are at least three neutrino mass eigenstates participating in the observed oscillation. Unfortunately, the most easily accessed signal for CP violation, $P(\nu_\mu \to \nu_{e,\tau}) \neq P(\overline{\nu}_\mu \to \overline{\nu}_{e,\tau})$, can be contaminated by the presence of "fake CP" asymmetries from the interactions of the beam with the matter of the earth [84]. A cleaner signature would be evidence of T violation from $P(\nu_\mu \to \nu_{e,\tau}) \neq P(\nu_{e,\tau} \to \nu_\mu)$, which would not be available to this generation of long baseline experiments.

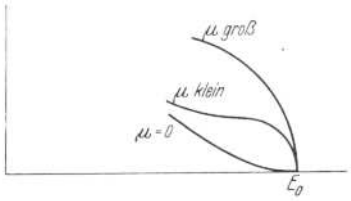

Figure 6: Electron spectrum at endpoint [86] for differing neutrino masses μ.

In the far future, some of the cleanest and most intense neutrino beams may come from a muon collider facility, either in the form of low energy beams from the muon source, or from $\mu^+ \to e^+ \nu_e \overline{\nu_\mu}$ decays. An analysis of a beam generated by decays in a 10 GeV muon storage ring and observed on the other side of the earth [85] shows an L/E reach $\sim 10^3$ km/GeV with a potential to probe low mixing probabilities even for modest muon production rates.

6.3 Kinematic Searches for Mass

Unlike searches for neutrino oscillations, kinematic searches are sensitive to non-zero neutrino masses in the absence of flavor or neutrino-antineutrino mixing. We discuss two important kinematic techniques which have placed stringent bounds on the $\overline{\nu}_e$ mass: β decay endpoint experiments, and the detection of neutrinos from Supernova 1987A.

The original method for measuring the electron neutrino mass relies on the precise measurement of the energy distribution of electrons emitted in β decay [86]. The number of counts as a function of electron energy E_e and momentum p_e is [87]

$$\frac{dN}{dE_e} \propto F(Z, E_e) p_e E_e (E_o - E_e) \sqrt{(E_o - E_e)^2 - M_\nu^2} \; . \tag{33}$$

Here, F is the Fermi function, Z the charge of the nucleus, and E_o the Q value of the decay neglecting the neutrino mass M_ν. The neutrino mass is extracted from the electron energy spectrum by fitting the endpoint region of the spectrum with M_ν^2 as a free parameter. The square of M_ν appears because the sensitivity to M_ν resides in the curvature of the spectrum at the endpoint rather than the zero crossing, Figure 6. The most sensitive experiments use the decay

$$^3H \to ^3He + e^- + \overline{\nu}_e \; , \tag{34}$$

which has an endpoint energy of 18.5901 ± 0.0017 keV [88]. This elegant method is hampered by low count rates in the endpoint region (if $M_\nu = 5$ eV, the fractional change in the total number of counts is 3×10^{-11}) and detector resolution, which tends to smear counts to higher energies, thus masking the effect of a massive neutrino.

Kinematic measurements require large sources and long running periods to accumulate statistics near the endpoint, and spectrometer energy resolutions better than 10 eV. In addition, atomic effects and electron energy loss in the source and spectrometer must be understood and accounted for at the few electron volt level [89]. Table 6 summarizes the measurements since 1990 and shows an asymptotic approach to $M_\nu \sim 1$ eV.

Experiment	ΔE (eV)	M_ν^2 (eV^2)	M_ν <(95% c.l.) (eV)
LANL [92]	23	$-148 \pm 68 \pm 41$	9.3
Zurich [93]	17	$-24 \pm 48 \pm 61$	11
Tokyo INS [94]	16	$-65 \pm 85 \pm 61$	13
Livermore [95]			8
160 eV range	18	$-72 \pm 41 \pm 30$	
900 eV range	18	-130 ± 20	
Mainz [96]			
137 eV range	6	$-39 \pm 35 \pm 14$	7.2
500 eV range	6	-117 ± 18	
137 eV range	6	$-22 \pm 17 \pm 17$	6
Troitsk [97]			
220 eV range	4.3	-22 ± 4.8	1.7
270 eV range	4.3	$-2.7 \pm 10.1 \pm 4.9$	4.5
170 eV range	3.7	$3.8 \pm 7.4 \pm 2.8$	4.4
Combined 94-6		$1.5 \pm 5.9 \pm 3.6$	3.8
Combined 94-7		$-2.1 \pm 3.7 \pm 2.3$	3

Table 6: Summary of most recent kinematic searches using tritium decay. ΔE is the experimental energy resolution at the endpoint. M_ν^2 is the value extracted from the fit for the endpoint data, and M_ν the limit from the extracted value given by the authors. For the Livermore, Mainz and Troitsk experiments, the results arising from fits to different energy ranges around the endpoint are given.

Somewhat disturbingly, the preponderance of the earlier experiments shows a systematic trend of $M_\nu^2 < 0$, indicating either a common systematic effect (for example in the calculation of the atomic corrections) [90] or a new physics effect [91]. The most recent results from the Troitsk and Mainz experiments somewhat mitigate this concern and give limits of $M_\nu < 3$ eV.

Both the Mainz and Troitsk experiments propose ambitious upgrades to probe the mass region below 1 eV in the next five years. Such measurements will begin to probe the mass region favored by the LSND result and, in concert with further searches for double beta decay, help resolve the properties of the electron neutrino. As illustrated in Figure 8, Section 7, the neutrino mass eigenstate coupled most strongly to the electron (ν_1 in Figure 8) may have a mass too small to be seen in ^{3}H β decay experiments. These experiments must then have negative results.

Another type of kinematic constraint can be obtained from the observation of a neutrino burst from a nearby supernova. Water Čerenkov detectors can detect the $\overline{\nu}_e$s in such a burst. Typical models predict a burst of > 10 MeV $\overline{\nu}_e$s concentrated in a ~ 5 second time window. By studying the observed spread of arrival times as a function of $\overline{\nu}_e$ energy in the detectors on earth, a constraint on the mass can be directly obtained. Such a burst was observed in the IMB [98] and Kamiokande II [99] detectors from SN1987A in the Large Magellanic Cloud at a distance of 52 kpc. Useful limits are complicated to obtain because of uncertainties in neutrino production models and because of the low statistics (8 events from IMB and 11 from Kamiokande II), but upper bounds of $M_\nu \lesssim 30$ eV from SN1987A were obtained from detailed analyses of the observations and

astrophysical constraints [100, 101]. With the improvements in both tonnage and energy thresholds of contemporary neutrino observatories, another happy occurrence like SN1987A may provide additional direct $\overline{\nu}_e$ mass constraints.

6.4 Double Beta Decay

Unique amoung neutrino experiments, neutrinoless double beta decay ($0\nu\beta\beta$) occurs only if the neutrino is not only massive but a Majorana particle [102]. $0\nu\beta\beta$, the transition $(N,Z)\rightarrow(N-2,Z+2)+e^-+e^-$, occurs in any case when the mass of the parent nucleus (N,Z) is greater than the mass of the daughter nucleus $(N-2,Z+2)$, but the experimentally most interesting cases are when the intermediate state $(N-1,Z+1)$ has a mass greater than that of the parent nucleus, supressing the single beta decay $(N,Z)\rightarrow(N-1,Z+1)+e+\nu$. Sensitivity to the Majorana mass arises because the righthanded antineutrino emitted in the first $n\rightarrow p+e^-+\overline{\nu}_e$ transition must be reabsorbed as a lefthanded neutrino in $\nu_e+n\rightarrow p+e^-$. This reabsorption requires that $\overline{\nu}_e=\nu_e$, and for helicity reasons is suppressed by a factor M_ν/E_ν, where E_ν is the energy of the neutrino in the intermediate state. As a result, the $0\nu\beta\beta$ lifetime is

$$\left(T_{1/2,0\nu\beta\beta}\right)^{-1}=G_{0\nu}|\mathcal{M}_{0\nu}|^2\langle M_\nu\rangle^2\ , \tag{35}$$

where

$$\langle M_\nu\rangle\ =\sum_i U_{ei}^2 M_i\ . \tag{36}$$

The neutrino mass eigenstates, whose masses are M_i, must now be Majorana particles. Righthanded charged currents may affect the decay rate, but nonvanishing neutrino mass is required for $0\nu\beta\beta$ to take place [103]. $G_{0\nu}$ is a phase space factor and $\mathcal{M}_{0\nu}$ is the nuclear matrix element. Two neutrino double beta decay ($2\nu\beta\beta$) may also take place as an allowed process, and

$$\left(T_{1/2,2\nu\beta\beta}\right)^{-1}=G_{2\nu}|\mathcal{M}_{2\nu}|^2 \tag{37}$$

gives the rate.

All experiments searching for $0\nu\beta\beta$ rely on the measurement of the total energy of the two final state electrons, which must equal the Q value of the decay: $T_{e_1^-}+T_{e_2^-}=Q$. Experiments fall into two broad catagories: calorimeteric searches and tracking searches[3]. Calorimetric experiments use very high energy resolution to search for a peak in the $T_{e_1^-}+T_{e_2^-}$ spectrum against a constant background caused primarily by the Compton scattering of energetic gamma rays from radioisotope contaminants in the experimental apparatus. For a detector with $N\times10^{23}$ $\beta\beta$ decay candidates, energy resolution ΔE (in keV), and B background counts per keV in measuring time t years, the halflife sensitivity is [87]

$$T_{1/2}\sim ln2\times10^{23}\ y\left(\frac{Nt}{B\Delta E}\right)^{1/2}\ . \tag{38}$$

The most sensitive experiments use enriched ^{76}Ge cryogenic detectors and attain total energy resolutions of 1.5 keV around $Q=2041$ MeV. Germanium [105,

[3]Radio chemical experiments, in which an excess of $\beta\beta$ daughters in old elemental deposits is used to measure the total $0\nu\beta\beta+2\nu\beta\beta$ rate, are an exception [104].

Isotope	Experiment	$T_{1/2,0\nu\beta\beta}$ (yr)	$\langle M_\nu \rangle_{u.l.}$(eV)
^{48}Ca	HEP Beijing [111]	$> 1.1 \times 10^{22}$, 68% c.l.	23-50
^{76}Ge	Heidelberg/Moscow [105]	$> 5.7 \times 10^{25}$, 90% c.l.	0.2-0.8
	IGEX [106]	$> 0.8 \times 10^{25}$, 90% c.l.	
^{82}Se	Irvine	$> 2.7 \times 10^{22}$, 68% c.l.	4-14
	NEMO 2 [112]	$> 9.5 \times 10^{21}$, 90% c.l.	
^{96}Zr	NEMO 2 [113]	$> 1.3 \times 10^{21}$, 90% c.l.	-
^{100}Mo	LBL [106]	$> 2.2 \times 10^{22}$, 68% c.l.	3-111
	UCI [114]	$> 2.6 \times 10^{21}$, 90% c.l.	
	Osaka [115]	$> 2.8 \times 10^{22}$, 90% c.l.	
	NEMO 2 [119]	$> 5 \times 10^{21}$, 90% c.l.	
^{130}Te	Milano [116]	$> 7.7 \times 10^{22}$, 90% c.l.	2-5
^{136}Xe	Caltech/PSI/Neuchatel [109]	$> 4.4 \times 10^{23}$, 90% c.l.	2-5
^{150}Nd	UCI [120]	$> 1.2 \times 10^{21}$, 90% c.l.	5-6

Table 7: Current experimental limits on $0\nu\beta\beta$ decay and upper limits on $\langle M_\nu \rangle$.

106, 107], CdTe [108] and Te [116] detectors have the source as the detection medium, giving an efficiency approaching 100% for a system with a large number of emitters (10^{26} in the case of the largest germanium experiment). Detectors of 10 kg reach background limits of a few counts per year, probing the lifetime range above 10^{25} yr.

Tracking type detectors identify both electrons via their ionization deposition in a tracking medium and use either the total energy deposition or the bending in a magnetic field (or both) to determine the energy of each electron. Identification of the two electrons provides a powerful disciminant against backgrounds from γ, α and β emitters in the apparatus. The use of ^{136}Xe [109, 110] as a fill gas in a tracking type system gives high efficiency for a large number of emitters (4×10^{25} in the case of the largest experiment) by using the source as the detection medium. Other experiments [111, 112, 117, 118, 119, 120, 115] suspend the $0\nu\beta\beta$ emitter in the tracking volume. This limits the size of the source, as the source must be thin enough for the electrons to escape without significant energy loss in the source material.

The most sensitive experiments currently probe the lifetime range of 10^{23} to 10^{25} years, as summarized in Table 7 for the most experimentally attractive isotopes. None yield an observation of $0\nu\beta\beta$ and extraction of an upper limit for $\langle M_\nu \rangle$ is hampered by the complexity in calculating $\mathcal{M}_{0\nu}$. Two general methods are used in the computation of this nuclear matrix element [121]: the shell model and the quasiparticle random phase approximation (QRPA). Both give comparable results at the factor of five level. The QRPA is sensitive to the particle-particle coupling, which is poorly known and must be extracted from positron decay experiments. In the allowed range, the QRPA calculations indicate $0\nu\beta\beta$ may be completely suppressed by the nuclear matrix elements in some cases. Use of both methods gives rough agreement for the observed $2\nu\beta\beta$ rates. Overall, the limit on $\langle M_\nu \rangle$ from $0\nu\beta\beta$ lies around $\langle M_\nu \rangle < 1$eV.

The present generation of operating experiments will achieve sensitivities of $T_{1/2,0\nu\beta\beta} \sim 10^{26}$ yr, or $\langle M_\nu \rangle \lesssim 0.3$ eV. Ambitious plans are underway to push this limit even further: the GENIUS [122] experiment seeks to probe $\langle M_\nu \rangle < 0.1$ eV

Oscillating Neutrinos	Required $\left\vert\delta M^2\right\vert$ (eV^2)
Solar	10^{-10} or 10^{-5}
Atmospheric	10^{-3} to 10^{-2}
LSND	10^{-1} to 10^{+1}

Table 8: Mass splittings required by the three hints of oscillation.

through the use of several tons of enriched ^{76}Ge detectors. The CUORE experiment will use a cryogenic TeO_2 detector to achieve very high energy resolutions for large masses [123]. If, for example, the neutrinos have a quasi-degenerate mass spectrum (see Section 7), the coming experiments may cast light on the Majorana nature of the neutrino.

7 NEUTRINO MASS SCENARIOS

We have discussed the fairly strong evidence for neutrino mass from the behavior of the atmospheric neutrinos, the major further hint of mass from the behavior of the solar neutrinos, and the unconfirmed additional hint from the LSND experiment. To what neutrino mass scenarios do these hints point?

For simplicity, one would like to assume that there are just three neutrinos of definite flavor, ν_e, ν_μ, and ν_τ, and just three corresponding neutrinos of definite mass, ν_1, ν_2, and ν_3. However, for simplicity, one would also like to assume that the solar, atmospheric, and LSND oscillations each involve just a single oscillation "frequency", δM^2. But when one makes the latter assumption, the inferred frequencies of the three oscillations cannot all be accommodated in terms of the masses of just three neutrino mass eigenstates. For, these frequencies are, as we have seen, approximately as summarized by Table 8. Now, if there are only three mass eigenstates ν_i, then there are only three different mass splittings $\delta M^2_{ij} \equiv M^2_i - M^2_j$, and these three splittings obviously satisfy

$$\sum_{\text{Splittings}} \delta M^2_{ij} = (M^2_3 - M^2_2) + (M^2_2 - M^2_1) + (M^2_1 - M^2_3) = 0\,. \qquad (39)$$

But, as we note from Table 8, the splittings required by the three oscillations are, respectively, of three different orders of magnitude. Thus, they cannot possibly add up to zero, as demanded by Eq. (39), no matter what sign we assign to each of them. Hence, the three oscillations cannot all be explained in terms of just three neutrinos. To accommodate all three of these oscillations under the assumption that each oscillation is described by a single δM^2, we must introduce (at least) a fourth neutrino. Since we know from the width of the Z boson that only three species of neutrinos have normal weak interactions, this extra, fourth neutrino must be a sterile neutrino ν_S [10].

Since no direct evidence for any sterile neutrino has been seen, one wonders whether the simple assumption that each oscillation involves but a single δM^2 is false. Suppose, for example, that there are only three neutrinos, with masses such that $M^2_3 - M^2_2 \equiv \delta M^2_{\text{Big}} \gg M^2_2 - M^2_1 \equiv \delta M^2_{\text{Small}}$. Could it be that the oscillation of the LSND neutrinos involves δM^2_{Big}, the flavor conversion of the solar neutri-

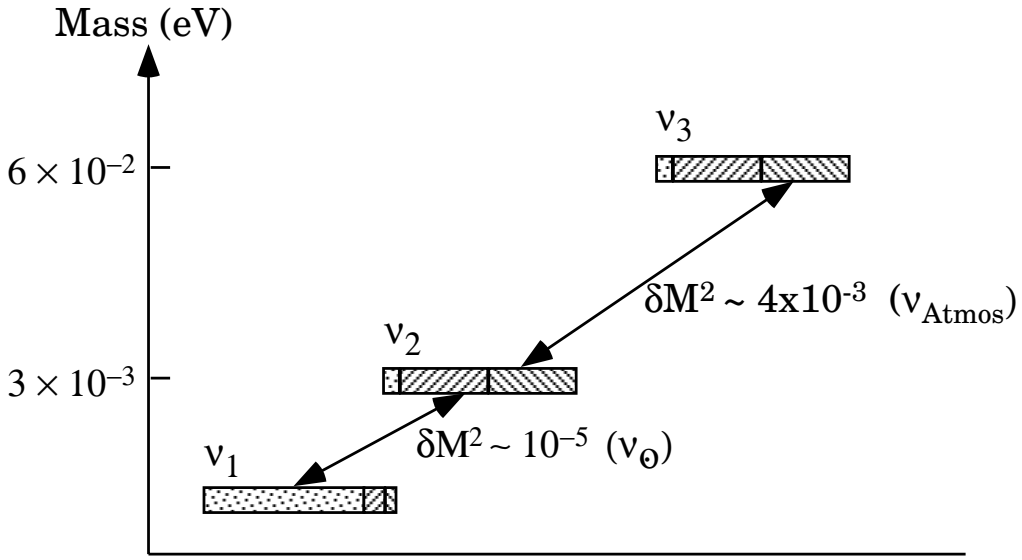

Figure 7: A three-neutrino mass hierarchy that accounts for the oscillations of atmospheric and solar neutrinos. The neutrinos ν_1, ν_2, and ν_3 are mass eigenstates. The rough flavor content of each of these is indicated by dotting and hatching: The ν_e fraction of a mass eigenstate is dotted, the ν_μ fraction is indicated by right-leaning hatching, and the ν_τ fraction by left-leaning hatching [125].

nos involves $\delta M^2_{\rm Small}$, and the oscillation of the atmospheric neutrinos involves a mixture of both $\delta M^2_{\rm Big}$ and $\delta M^2_{\rm Small}$? Then an analysis of the atmospheric data assuming (erroneously) that only one δM^2 is involved might find a value intermediate between those corresponding to the LSND and solar effects, as observed. Nevertheless, in this scenario, there are only three underlying neutrinos.

A number of analyses have attempted to exploit this possibility [124]. These attempts are clearly important, and should continue. However, the present authors have not seen any attempt to describe all three oscillations with just three neutrinos which is not at least somewhat inconsistent with some of the data. This being the case, we assume here that if one is to describe all three of the oscillations, at least four neutrinos are needed.

If one is reluctant to introduce a (light) sterile neutrino, then he can proceed by provisionally setting aside the so-far unconfirmed LSND oscillation, and attempting to explain only the atmospheric and solar neutrino data in terms of oscillation. One can then have the three-neutrino mass spectrum depicted in Figure 7, which assumes the behavior of the solar neutrinos is due to the small-angle MSW effect. The masses of the neutrinos in Figure 7 form a hierarchy, with $M_3 \gg M_2 \gg M_1$. The splitting $M_3^2 - M_2^2 \simeq M_3^2 \simeq 4 \times 10^{-3}{\rm eV}^2$ gives the atmospheric neutrino oscillation, while the splitting $M_2^2 - M_1^2 \simeq M_2^2 \simeq 10^{-5}\,{\rm eV}^2$ yields the MSW effect in the sun.

The hierarchy in Figure 7 is the lightest one which gives the δM^2 values called for by the atmospheric and solar oscillations. Since oscillations determine only mass splittings, and not actual masses, one, of course, can increase the masses in Figure 7 without affecting the oscillations so long as one keeps the δM^2 values fixed. For example, if neutrinos contribute significantly to Ω_M, then perhaps

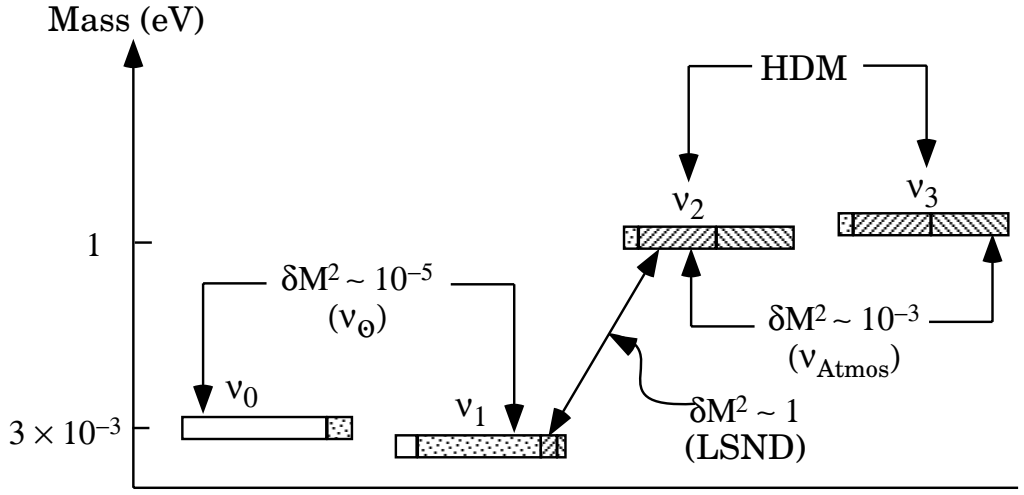

Figure 8: A four-neutrino scenario that accounts for the oscillations of the atmospheric, solar, and LSND neutrinos. The scenario contains the mass eigenstates $\nu_0 - \nu_3$. The ν_e, ν_μ, and ν_τ fractions of these mass eigenstates are indicated as in Figure 7, and the ν_S fraction is shown as a clear region. The mass eigenstate ν_0 is largely a sterile neutrino ν_S. The ~ 1 eV neutrinos in the scheme make a significant contribution to Hot Dark Matter.

we have a quasi-degenerate neutrino mass spectrum with $M_1 \simeq M_2 \simeq M_3 \simeq (1-2)$ eV and the splittings δM^2 as in Figure 7.

Suppose the behavior of the solar neutrinos is due to oscillation in vacuum, rather than to the MSW effect. Then the masses of the neutrinos in Figure 7 must be changed to give the small δM^2 ($\sim 10^{-10}\text{eV}^2$) that corresponds to solar neutrino vacuum oscillations. Also, their flavor content must be changed to reflect large solar neutrino mixing ($\sin 2\theta \sim 0.8$). However, a neutrino mass-and-mixing scenario that corresponds to the solar and atmospheric observations is easily obtained [126].

If one is willing to include a ν_S among the light neutrinos, then all three hints of oscillation can be accommodated. One neutrino mass scenario which accommodates them is shown in Figure 8 [127]. In this scenario, the mass spectrum includes two ~ 1 eV mass eigenstates, ν_2 and ν_3, split by a $\delta M^2 \sim 10^{-3}$ eV^2 that produces the atmospheric neutrino oscillation. It also includes two much lighter mass eigenstates, ν_0 and ν_1, split by a $\delta M^2 \sim 10^{-5}$ eV^2 that yields the MSW effect in the sun. However, as we see from Figure 8, in this scheme the MSW effect converts a ν_e into the largely sterile neutrino ν_0 rather than into a ν_μ or ν_τ. Thus, there is no ν_μ or ν_τ component in the solar neutrino flux. Finally, the splitting $\delta M^2 \sim 1$ eV^2 between the heavy pair ν_2 and ν_3, and the light pair ν_0 and ν_1, produces the LSND oscillation. The heavy pair in this scenario has been given the smallest average mass, $\sim$ 1eV, which can still yield the $\delta M^2 \sim 1$ eV^2 called for by LSND. Interestingly, with this ~ 1 eV mass, the members of the pair make a significant Hot Dark Matter contribution to the mass density of the universe, but without violating the cosmological upper bound of Eq. (31) on neutrino mass.

In a theory containing the see-saw mechanism for neutrino mass, a sterile neutrino occurs naturally, as we have seen in Section 2. However, this sterile

neutrino is very heavy, with a mass in the multi-GeV range or higher. In general, theories of neutrino mass do not predict *light* sterile neutrinos, such as the one in Figure 8. However, even if one does not include LSND, the large mixing angles observed in atmospheric, and perhaps solar, neutrino oscillation also suggest that light sterile neutrinos may exist. The small mixing angles observed in the quark sector of the Standard Model lead us to expect naively that the mixing angles between active species of neutrinos are also small. However, there would be no such expectation for mixing between active and sterile neutrinos. Indeed, appealing theories have been constructed in which, as a result of a symmetry, the mixing between an active neutrino and a sterile one is automatically maximal [128].

Firm establishment of the existence of a light sterile neutrino would be a groundbreaking result. Thus, it is very important to confirm or disprove each of the three present hints of oscillation, and to thoroughly examine the question of whether or not these three oscillations, if all confirmed, together require the existence of a fourth, sterile neutrino. It is also important to carry out experiments which can tell whether solar or atmospheric neutrino oscillation, or both, involve a sterile neutrino.

The neutrino-mass scenarios we have discussed are just examples. Other scenarios are possible [126]. As discussed in our concluding section, the various neutrino mass and mixing possibilities will be tested through future experiments.

8 CONCLUSIONS

To conclude this breathless sprint through the rich world of neutrino oscillation and neutrino mass physics, we consider the possible paths through the maze of revealing measurements that are expected in the next five or ten years and where this information might point experimenters and theorists in the long term. Some of the mainstream experimental questions to be answered are summarized in Table 9. *Caveat emptor*: if the rapid changes in our knowledge in the past ten years is any indication, the phase space for surprises outside of the scope of these questions may be large. We consider, in turn, probes of our three neutrino oscillation hints: solar neutrinos, atmospheric neutrinos and the LSND signal.

The low δM^2 expected to be responsible for the flavor conversion of solar neutrinos precludes accelerator-based probes of this signal in the near future. However, on the observational front, both SNO and BOREXINO will begin data taking. BOREXINO will measure the ^{7}Be flux and search for seasonal variations in the solar neutrino flux. Observation of a deep deficit of ^{7}Be flux would indicate that solar neutrinos oscillate according to the small angle MSW solution or in vacuum. This would be confirmed by the observation at SNO or SuperKamiokande of a deviation from the neutrino energy distribution in the absence of oscillations. Observation of a seasonal variation at BOREXINO would mean the oscillation depends on the earth-sun distance, indicating vacuum oscillations play a role in solar neutrino behavior. Perhaps the most exciting probe is SNO's measurement of the neutral current solar neutrino interactions. Muon and tau neutrinos have neutral current interactions of the same strength as electron neutrinos. Thus, if the missing solar electron neutrinos oscillate into another active neutrino flavor, either muon or tau, the rate for neutral current interactions of solar neutrinos will be the same as in the absence of oscillation. However, if the missing elec-

Future observation	Solar ν oscillation	Atmospheric ν oscillation	LSND ν oscillation
~ 1 eV ν_e in tritium decay	If solar ν osc., then at least 2-fold degeneracy with $\delta M^2 < 10^{-5}$	-	δM^2 gives us masses of two eigenstates
$0\nu\beta\beta$ at $\sim$ 0.1eV ($\Rightarrow \nu = \overline{\nu}$)	-	May be relevant	$\nu_e \rightarrow \overline{\nu_e}$ contributes?
SNO NC/CC as expected	Solar $\nu_e \rightarrow \nu_\mu$ or ν_τ	NC deficit implies only one ν_s which participates here	-
SNO NC/CC deficit	dN/dE_ν distortion proves oscillations, and therefore ν_s	NC deficit here implies another ν_s	-
Deep BOREXINO ^{7}Be deficit	Big dN/dE_ν distortion confirms small angle MSW	-	-
BOREXINO seasonal variation	ν_e vacuum oscillations	-	-
$\overline{\nu}_e$ disappearance in KAMLAND	Large angle MSW (day/night or small dN/dE_ν distortion would confirm)	-	-
Results of long baseline experiments (MINOS, K2K, CERN)	-	Confirm $\nu_\mu \rightarrow \nu_\tau$ if see τ appearance	-
Confirmation and measurement of LSND δM^2 by BooNe, I-216	Three signatures suggest three distinct mass splittings, and thus a fourth light (sterile) neutrino needed		

Table 9: Some possible outcomes of future observations are listed. Next to each possible outcome are listed consequences or provocative additional experimental signatures related to the solar, atmospheric or LSND neutrino oscillations.

tron neutrinos are oscillating into sterile neutrinos, the neutral current rate will be reduced. If such a reduced rate is observed and if additional confirmation of the oscillation hypothesis for solar neutrino disappearance is obtained, such as a large day/night effect or anomalous solar neutrino energy spectrum, the case for $\nu_e \to \nu_s$ oscillations will become increasingly compelling. If the large angle MSW solution is indicated by small distortions of the solar neutrino energy spectrum and a large day/night effect, then the KAMLAND reactor experiment will take center stage with the first possibility for a terrestrial confirmation of the solar neutrino oscillation hypothesis.

The path to verifying the oscillation hypothesis for the atmospheric neutrino anomaly seems to clearly point to the next generation of long-baseline accelerator experiments, MINOS, K2K and CERN to Gran Sasso. Unless δM^2 is at the lowest end of the range suggested by the SuperKamiokande data, all three programs should have access to observing the ν_μ oscillations; however, since L/E in all these experiments gives a peak sensitivity at $\delta M^2 \sim 10^{-2}$, there is a significant possibility that these experiments will not be able to measure δM^2 by observing a complete oscillation cycle. Therefore, a low δM^2 may require either substantial beam redesign or a different baseline, which may in turn drive a new generation of long-baseline experiments. Since the reactor oscillation experiments (and the SuperKamiokande data itself) rule out the $\nu_\mu \to \nu_e$ interpretation of the atmospheric data, a premium is placed on the ability to detect τ's or neutral current ν_τ interactions in order to determine whether the atmospheric neutrinos oscillate to ν_τ or to a sterile neutrino. Here, the higher energy experiments, MINOS and the CERN-Gran Sasso beam, will have an advantage over K2K, which cannot produce τ leptons. Should CP violation in neutrino oscillations be observed in these long baseline experiments, this would imply that at least three neutrino mass eigenstates have splittings, δM^2, large enough to be within the sensitivity of these experiments. This could be interpreted within the three neutrino framework as favoring an explanation for the solar neutrino deficit other than oscillation with a very small $deltaM^2$, or it could imply the presence of a fourth, sterile neutrino.

New experiments, BooNE at Fermilab and I-216 at CERN, should be able to conclusively confirm or refute the LSND signal, and measure δM^2 and the mixing if the effect is observed. If the effect persists, it is possible the electron neutrino lies within the reach of a kinematic measurement. Kinematic techniques must be employed in order to resolve the overall scale of neutrino masses since oscillation is only sensitive to splittings. At this time, the best one can hope for is a mass sensitivity of 0.1 eV for ν_e, which would begin to probe mass splittings favored by the LSND result. If the electron neutrino were shown to have a mass ~ 0.1 eV, the solar neutrino oscillation would indicate there are two nearly mass degenerate neutrinos with $\delta M^2 < 10^{-5}$ eV^2. A very interesting and important experiment would be one which could resolve ν_μ or ν_τ masses at the $\delta M^2 \sim 1$ eV^2 level.

The Majorana or Dirac nature of the neutrino remains an open question. We can hope for a mass sensitivity of 0.1 eV for Majorana electron neutrinos in the coming years which, if observed, indicates the LSND oscillation could be at least partially attribtued to $\nu_e \to \overline{\nu_e}$. Direct probes of the question of the Majorana nature of the other neutrinos is likely to be unresolved for the forseeable future.

Implicit in many of these outcomes is very exciting physics beyond the Standard Model. The survival of all three current hints, discovery of CP violation inconsistent with only three neutrinos, or direct probes for solar or atmospheric

neutrino "disappearance" may indicate the presence of a new particle, a light sterile neutrino. Understanding its relationship to our current picture of exactly three generations of quarks, leptons and light neutrinos will prove a major challenge, both theoretically and experimentally, as the generational structure of fermions is probed at the energy frontier of accelerator experiments.

In summary, current experimental results strongly indicate neutrinos have mass and the different lepton flavors mix. While lepton family number appears to be violated, the question of total lepton number conservation remains open. Currently-operating and soon-to-start experiments will take important steps toward completing the neutrino picture, but some large issues most likely will not soon be resolved. We expect that neutrino physics will remain a central focus of both experimental and theoretical endeavor for a long time to come.

Acknowledgements

We would like to thank John Bahcall, Robert Bernstein, Felix Boehm, David Caldwell, Martin Deutsch, George Fuller, Tom Gaisser, Steve Geer, Maury Goodman, Giorgio Gratta, Donald Groom, John Learned, Eugene Loh, John LoSecco, Bill Louis, Geoff Mills, Stephen Parke, Serguey Petcov, Jon Rosner, Henry Sobel, Jack Steinberger, Petr Vogel and Lincoln Wolfenstein for helpful and stimulating discussions during the formulation of this review. We owe a special debt to Susan Kayser for her heroic efforts in helping to prepare this document. One of us (BK) would like to acknowledge the hospitality of the Aspen Center for Physics where there were many opportunities to exchange ideas about neutrino mass. This work was supported by the US Department of Energy and the Alfred P. Sloan Foundation.

Literature Cited

1. Gell-Mann M, Ramond P, Slansky R. In *Supergravity*, eds. D Freedman, P van Nieuwenhuizen, p. 315. Amsterdam: North Holland (1979); Yanagida T. In *Proceedings of the Workshop on Unified Theory and Baryon Number in the Universe*, eds. O Sawada, A Sugamoto. Tsukuba, Japan: KEK (1979); Mohapatra R, Senjanovic G. *Phys. Rev. Lett.* 44:912 (1980) and *Phys. Rev.* D23:165 (1981)
2. Kayser B. Neutrino Mass. In Caso C, Conforto G, Gurtu A, Aguilar-Benitez M, Amsler C, *et al. Eur. Phys. J.* C3:1 (1998)
3. Kayser B, Stodolsky L. *Phys. Lett.* B359:343 (1995)
4. Srivastava Y, Widom A, Sassaroli E. *Z. Phys.* C66:601 (1995)
5. Kayser B. *Phys. Rev.* D24:110 (1981); Boehm F, Vogel P. *Physics of Massive Neutrinos*, p. 87. Cambridge: Cambridge University Press (1987); Giunti C, Kim C, Lee U. *Phys. Rev.* D44: 3635 (1991); Rich J. *Phys. Rev.* D48:4318 (1993); Lipkin H. *Phys. Lett.* B348:604 (1995); Grimus W, Stockinger P. *Phys. Rev.* D54:3414 (1996); Goldman T. eprint hep-ph/9604357; Grossman Y, Lipkin H. *Phys. Rev.* D55:2760 (1997)
6. Stodolsky L. *Phys. Rev.* D58:036006 (1998); Lipkin H. eprint hep-ph/9901399; Grimus W, Mohanty S, Stockinger P. eprint hep-ph/9904340
7. Cabibbo N. *Phys. Lett.* 72B:333 (1978)
8. For recent analyses of CP violation in neutrino oscillation, see Gago AM, Pleitez V, Funchal RZ. eprint hep-ph/9810505; Schubert KR. eprint hep-ph/9902215; Dick K, Freund M, Lindner M, Romanino A. eprint hep-ph/9903308; Bernabeu J. eprint hep-ph/9904474
9. This quantity has a simple geometrical meaning; see Jarlskog C. In *CP Violation*, ed. C Jarlskog, p.3. Singapore: World Scientific (1989)
10. Otherwise, the Z would decay into pairs of these additional neutrinos, and we know that it does not do so. See Karlen D. The Number of Light Neutrino Types, from Collider

Experiments. In Caso C, Conforto G, Gurtu A, Aguilar-Benitez M, Amsler C, *et al. Eur. Phys. J.* C3:1 (1998)
11. See, for example, Kayser B, Gibrat-Debu F, Perrier F. *The Physics of Massive Neutrinos.* Singapore: World Scientific (1989)
12. Schröder H. In *B Decays* (Revised Second Edition), ed. S Stone, p. 449. Singapore: World Scientific (1994); Wu SL. *Proc. 17th Int. Symp. on Lepton-Photon Interactions, 1995*, eds. Zheng Zhi-Peng, Chen He-Sheng, p.273. Singapore: World Scientific (1996)
13. Bilenky S, Pontecorvo B. *Lett. Nuovo Cimento* 17:569 (1976); Barger V, Langacker P, Leveille JP, Pakvasa S. *Phys. Rev. Lett.* 45:692 (1980); Bilenky SM, Hosek J, Petcov ST. *Phys. Lett.* B94:495 (1980); Schechter, J, Valle JWF. *Phys. Rev.* D22:2227 (1980); Cheng TP, Li LF. *Phys. Rev.* D22:2860 (1980); Yanagida T, Yoshimura M. *Progr. Th. Phys.* 64:1870 (1980); Kobzarev IYu *et al. Sov. J. Nucl. Phys.* 32:823 (1980)
14. Langacker P, Wang J. *Phys. Rev.* D58:093004 (1998)
15. Wolfenstein L. *Phys. Rev.* D17:2369 (1978), *Phys. Rev.* D20:2634 (1979); Mikheyev SP, Smirnov AYu. *Sov. J. Nucl. Phys.* 42:913 (1986), *Sov. Phys.* -JETP64:4 (1986), *Nuovo Cimento* 9C:17 (1986)
16. Honda M, *et al. Phys. Rev.* D52:4985 (1995) ; Honda M, *et al. Phys. Lett.* B248:193 (1990); Bar G, *et al. Phys. Rev.* D39:3532 (1989) ; Agrawal V *et al. Phys. Rev.* D53:1314 (1996) ; Gaisser T, Proc. 24th International Cosmic Ray Conference (Rome) v1:694 (1995)
17. Loh E. Private communication
18. Barger V, Learned JG, Pakvasa S, Weiler TJ. *Phys. Rev. Lett.* 82:2640 (1999); Lipari P, Lusignoli M. *Phys. Rev.* D60:013003 (1999); Fogli GL, Lisi E, Marrone A, Scioscia G. eprint hep-ph/9902267; Choubey S, Goswami S. *Phys. Rev* D59:117303 (1999)
19. Agleilta M, *et al. Europhys. Lett.* 8:611 (1989)
20. Allison W, *et al. Phys. Lett.*B391:491 (1997)
21. Becker-Szendy R, *et al. Phys. Rev.* D46:3720 (1992) ; Caspar D, *et al. Phys. Rev. Lett.* 66:2561 (1991)
22. Berger Ch, *et al. Phys. Lett.* B277:489 (1989)
23. Takita, M., Tsukuba KEK - KEK-88-010.
24. Fukuda Y, *et al. Phys. Lett.* B335:237 (1994)
25. Fukuda Y, *et al. Phys. Rev. Lett.* 81:1562 (1998)
26. Kasuga S *et al. Phys. Lett.* B374:238 (1996)
27. Fukuda Y, *et al. Phys. Lett.* B436:33 (1998)
28. Fukuda Y, *et al. Phys. Lett.* B433:9 (1998)
29. Meisser M, "Atmospheric Neutrinos at SuperKamiokande", in proccedings of DPF '99
30. Vannucci F, hep-ph/9903487
31. Lipiri P, *et al.* astro-ph/9803093
32. Futagami T, *et al.* astro-ph/9901139
33. Allison W, *et al. Phys. Lett.* B449:137 (1999)
34. D. Kielczewska *et al.* [IMB Collaboration], "Flavour composition of atmoshperic neutrinos measured in IMB-3 detector". In *Villars sur Ollon, Perspectives in neutrinos, atomic physics and gravitation* 219-225 (1993)
35. Hiata KS, *et al. Phys. Lett.* B280:146 (1992)
36. Fikuda Y, *et al. Phys. Rev. Lett.* 82:2644 (1999)
37. Ambrosio M, *et al. Phys. Lett.* B434:451 (1998)
38. For an excellent introduction, see *Neutrino Astrophysics*, John N Bahcall, Cambridge University Press, 1989. A more recent review is given in Bahcall JN, hep-ph/9711358
39. Bahcall JN, Krastev PI, and Smirnov Yu, *Phys. Rev.* D58:096016 (1998)
40. An excellent collection of figures and explanations of solar neutrino physics may be found at http://www.sns.ias.edu/$\tilde{}$jnb
41. Losecco JM, *et al. Phys. Lett.* B184:305 (1987)
42. Fukuda Y, *et al. Phys. Rev. Lett.* 81:1158 (1998)
43. Fukuda Y, *et al. Phys. Rev. Lett.* 82:2430 (1999)
44. Cleveland BT, *et al. Astrophys. J.* 496:505 (1998)
45. Abdurashitov JN, *et al. Phys. Rev. Lett.* 77:4708 (1996)
46. Hampel W, *et al. Phys. Lett.* B447:127 (1999)
47. Abdurashitov JN, *et al. Phys. Rev. Lett.* 59:2246 (1999); Bernabei R, *et al. Nucl. Phys. Proc. Suppl.* 48:304 (1996)
48. Bahcall JN, Basu S, Pinsonneault MH. *Phys. Lett.* B433:1 (1998)

49. SuperKamiokande preprint, Jan. 26, 1999, submitted to *Phys. Rev. Lett.*. Available from http://www-sk.icrr.u-tokyo.ac.jp/doc/sk/pub/index.html
50. The day/night distinction could be significantly enhanced for neutrinos passing through the earth's core. See Maris M, Petcov ST. *Phys. Rev.* D58:113008(1997); Petcov ST. *Phys. Lett.* B434:321 (1998); Akhmedov EKh. eprint hep-ph/9903302; Chizhov MV, Petcov ST. eprint hep-ph/9903399
51. Okada C, "Status of SNO", In proceedings of DPF '99.
52. G. Alimonti *et al. Nucl. Phys. Proc. Suppl.* 32:149 (1998)
53. Athanassopoulos C, *et al. Phys. Rev. Lett.* 77:3082 (1996); Athanassopoulos C, *et al. Phys. Rev.* C54:2685 (1996)
54. Athanassopoulos C, *et al. Phys. Rev. Lett.* 81:1774 (1998); Athanassopoulos C, *et al. Phys. Rev.* C58:2511 (1998)
55. Bergmann S, and Grossman Y hep-ph/9808524; Johnson LM, and McKay DW. *Phys. Lett.* B433:355 (1998); Adhikari R, and Omanovic, G., *Phys. Rev.* D59:073003 (1999)
56. Eitel K, *et al.* (1998)
57. R. Maschuw, private communication
58. Harris D, *et al.* Neutrino Oscillations at NuTeV", proceedings of DPF '99, preprint UR-1568.
59. Romosan A, *et al.Phys. Rev. Lett.* 78:2912 (1997)
60. Altegoer J, *et al.* Contributed Paper to Lepton-Photon Conference, July 1997
61. Ahrens L, *et al. Phys. Rev.* D36:702 (1987)
62. Borodovsky L, *et al. Phys. Rev. Lett.* 68:274 (1992)
63. Church E, *et al.* FERMILAB-P-0898
64. Armenise N, *et al.* CERN-SPSC/97-21
65. Bahcall N, Fan X. *Proc. Natl. Acad. Sci. USA* 95:5956 (1998)
66. We thank Neta Bahcall, Joel Primack, and Gary Steigman for illuminating and detailed discussions of the mass density of the universe, and the possible contribution of Hot Dark Matter
67. Kolb EW, Turner MS. *The Early Universe*. Redwood City, CA: Addison-Wesley (1990)
68. Reines F, Cowan CL, *Phys. Rev.* 113:1 (1959)
69. Zacek G, *et al. Phys. Rev.* D34:2621 (1986); Cavaignac J-F, *et al. Phys. Lett.* B148:387 (1984)
70. Vogel P, *et al. Phys. Rev.* C24:1543 (1981); Klapdor HV, *et al. Phys. Lett.* B112:22 (1982); Schreckenbach K, *et al. Phys. Lett.* B160:325 (1985)
71. Apollonoio . *Phys. Lett.* B420:397 (1998)
72. Boehm F, *et al.*, *Prog. Art. Nucl. Phys* 40:253 (1998)
73. Gratta G. "Neutrino Oscailltion Experiments at Nuclear Reactors" In the proceedings of 17th International Workshop on Weak Interactions and Neutrinos (WIN 99), Cape Town, South Africa, 24-30 Jan 1999
74. Derbin Ya, *Phys.Atom.Nucl.* 57:222 (1994)
75. Broggini C, "Status of the MUNU experiment ". In Proceedings of Topics in Astroparticle and Underground Physics, LNGS, Italy, 1997
76. Goodman M, "Prospects for Long-Baseline Neutrino Oscillation Experiments". In the *Proceedings of the Workshop on Long-Baseline Neutrino Oscillation*, Fermilab, 17-20 November (1991)
77. Eskut E, *et al. Phys. Lett.* B434:205 (1998)
78. Altegoer J, *et al.Phys. Lett.* B431:219 (1998)
79. Ables E, *et al.* "Main Injector Neutrino Oscillation Search", FERMILAB-PROPSAL-P-875 (1995)
80. Nishikawa K, *et al.* "E362 KWK-PS proposal", March 1995; *Nucl. Phys. (Proc. Supp.)* B59:289 (1997)
81. Rubbia A, *et al.* CERN-SPSLC-96-58 (1996)
82. Ambrosio M, *et al.* INFN-AE-98-09 (1998)
83. CERN/SPSC-98-25 (1998).
84. Ref. [8], Bernabeu J.
85. Geer S, *Phys. Rev.* D57:6989 (1998)
86. Fermi E, *Zeit. Phys.* 88: (1934)161.
87. Boehm F and Vogel P, *Physics of Massive Neutrinos*, Cambridge University Press, 1987 [See Ref. [5]]

88. Van Dyck RS, *et al. Phys. Rev. Lett.* 70:2888 (1993)
89. Fackler O, *et al. Phys. Rev. Lett.* 55:1388 (1985)
90. See, for example, Rizek J, *et al. Phys. Lett.* B440:89 (1998)
91. Stephenson GJ, *et al.* nucl-th/9807057; Lobashev VM, "Neutrino Mass and Anomaly in the Tritium Beta Spectrum". In Proceedings The XVIIIth InternationalConference on Neutrino Physics and Astrophysics (NEUTRINO'98) Takayama, Japan on 4-9 June, 1998.
92. Robertson RGH, *et al. Phys. Rev. Lett.* 67:957 (1991)
93. Holzschuh, *et al. Phys. Lett.* B287:381 (1992)
94. Kawakami H, *et al. Phys. Lett.* B256:105 (1991)
95. Sotefffl W, A. Decman, *Phys. Rev. Lett.* 75:3237 (1995)
96. Weinheimer Ch, *et al. Phys. Lett.* B300: (1993) 210; Weinheimer Ch, "Results from the Mainz Neutrino Mass Experiment". In Proceedings The XVIIIth InternationalConference on Neutrino Physics and Astrophysics (NEUTRINO'98) Takayama, Japan on 4-9 June, 1998.
97. Belesev A., *et al. Phys. Lett.* B350:263 (1995)
98. Bionta RM, *et al. Phys. Rev. Lett* 58:1494 (1987)
99. Hirata K, *et al. Phys. Rev. Lett* 58:1490 (1987)
100. Kolb EW, Stebbins AJ, Turner MS. *Phys. Rev.* D35:3598 (1987)
101. Abbott LF, DeRujula A, Walker TP. *Nucl. Phys.* B299:734 (1988)
102. Primakov H, Rosen SP. *Rep. Prog. Phys.* 22:121 (1969)
103. Schechter J, Valle J. *Phys. Rev.* D25:2951 (1982); Takasugi E. *Phys. Lett.* 149B:372 (1984); Kayser B. In *Proceedings of the Seventh Moriond Workshop on New and Exotic Phenomena* eds. O Fackler, J Tran Thanh Van, p. 349. Gif-sur-Yvette, France: Editions Frontieres (1987); Bilenky S, Petcov S. *Rev. Mod. Phys.* 59:671 (1987); Kayser B. In *Proceedings of the XXVI International Conference on High Energy Physics* ed. J Sanford, p. 1153. New York: American Institute of Physics (1993); Rosen SP. In *Proceedings of the Franklin Symposium in Celebration of the Discovery of the Neutrino* eds. C Lane, R Steinberg, p. 31. Singapore: World Scientific (1993)
104. Kirsten T, *Phys. Rev. Lett.* 50:474 (1983) and *Z. Physik* C16:189 (1983)
105. Baudis L, *et al.* hep-ex/9902014
106. Morales A, "Review on Double Beta Decay Experiments and Comparison with Theory". In proceedings of 18th International Conference on Neutrino Physics and Astrophysics (NEUTRINO 98), Takayama, Japan, 4-9 Jun 1998.
107. Caldwell DO, *et al. Nucl. Phys. B Proc. Suppl.* 13:547 (1990); Reusser D, *et al. Phys. Rev.* D45:2548 (1992)
108. Danevich FA, *et al. Phys. Lett.* B344:72 (1995) ; Mitchell, LW and P Fisher, *Phys. Rev.* C192:895 (1988)
109. Vuilleumier L, *et al. Phys. Rev.* D48:1009 (1993); Farine J, *et al. Phys. Lett.* B434:407 (1998)
110. Bellotti, E, *et al. Phys. Lett.* B266:193 (1991)
111. You, K, et al., *Phys. Lett* B265:53 (1991)
112. Arnold, R *et al.*, *Nucl. Phys.* A636:209(1998)
113. Barahbash, A *et al.*, *Nucl. Phys.* A629:517c(1998)
114. Moe, M, MA Nelson, M Vient, *Prog. Part. Nucl. Phys.* 32:247(1994)
115. Watanabe, T, *et al.*, J̃. Phys. G17:S217 (1991)
116. Alessandrello, A, *et al. Phys. Lett.* B433:156 (1998)
117. Balysh A, *et al. Phys. Rev. Lett.* 77:5186 (1996)
118. De Silva A, *et al. Phys. Rev.* C56:2451 (1997)
119. Dassie D, *et al. Phys. Rev.* D51:2090 (1995)
120. Artemev VA, *et al. Phys. Lett.* B345:564 (1995)
121. For a recent review, see Faessler A and F Simkovic, hep-ph/9901215 or Vogel P and M Moe, *Ann. Rev. Nucl. Part. Phys.* 44:247 (1994).
    See also Caurier E, *et al. Phys. Rev. Lett.* 77:1954 (1996); Engel J, *et al. Phys. Rev.* C 37:731 (1988); Tomoda T., *Rep. Prog. Phys.* 54:53 (1991); Simkovic F, *et al. Phys. Lett.* B393:267 (1997)
122. Klapdor-Kliengrothaus HV, *et al.* hep-ex/9901021
123. Cermonesi O., invited talk, Neutrino 98.
124. Teshima T, Sakai T, Inagaki O. eprint hep-ph/9801276; Teshima T, Sakai T. *Prog. Theor. Phys.* 101:147 (1999); Thun RP, McKee S. *Phys. Lett.* B439:123 (1998); Barenboim G,

Scheck F. *Phys. Lett.* B440:332 (1998); Sakai T, Teshima T. eprint hep-ph/9901219; Ohlsson T, Snellman H. eprint hep-ph/9903252

125. We owe this general approach to depicting neutrino-mass scenarios to Smirnov A, in *Proc. 28th Int. Conf. on High Energy Physics,* eds. Z Ajduk and A Wroblewski, p. 288. Singapore: World Scientific (1997)
126. See, for example, Smirnov AYu. eprint hep-ph/9901208, and references therein
127. This is a somewhat modified version of a neutrino-mass scenario proposed by Caldwell D, Mohapatra R. *Phys. Rev.* D48:3259 (1993). See also Peltoniemi JT, Tommasini D, Valle JWF. *Phys. Lett.* B298:383 (1993); Barger V, Pakvasa S, Weiler T, Whisnant K. *Phys. Rev.* D58:093016 (1998)
128. Foot R, Volkas RR. *Phys. Rev.* D52:6595 (1995). See also Brahmachari B, Mohapatra R. *Phys. Lett.* B437:100 (1998); Mohapatra R. eprint hep-ph/9903261